FINAL REPORT

Environmentally Preferred and Improved (Rapid) Laser Coating Removal Process for the Safe Removal of Coatings from Composite Substrates

ESTCP Project WP-201709

Connor Eviston
Air Force Life Cycle Management Center

Hannah Easton
University of Dayton Research Institute

Andy Strat
Titan Robotics

30 September 2020

DISTRIBUTION STATEMENT A.
Approved for public release: distribution unlimited.

REPORT DOCUMENTATION PAGE

Form Approved
OMB No. 0704-0188

The public reporting burden for this collection of information is estimated to average 1 hour per response, including the time for reviewing instructions, searching existing data sources, gathering and maintaining the data needed, and completing and reviewing the collection of information. Send comments regarding this burden estimate or any other aspect of this collection of information, including suggestions for reducing the burden, to Department of Defense, Washington Headquarters Services, Directorate for Information Operations and Reports (0704-0188), 1215 Jefferson Davis Highway, Suite 1204, Arlington, VA 22202-4302. Respondents should be aware that notwithstanding any other provision of law, no person shall be subject to any penalty for failing to comply with a collection of information if it does not display a currently valid OMB control number.
PLEASE DO NOT RETURN YOUR FORM TO THE ABOVE ADDRESS.

1. REPORT DATE *(DD-MM-YYYY)*
30/09/2020

2. REPORT TYPE
ESTCP Final Report

3. DATES COVERED *(From - To)*

4. TITLE AND SUBTITLE
Environmentally Preferred and Improved (Rapid) Laser Coating Removal Process for the Safe Removal of Coatings from Composite Substrates

5a. CONTRACT NUMBER

5b. GRANT NUMBER

5c. PROGRAM ELEMENT NUMBER

6. AUTHOR(S)
Connor Eviston, Air Force Life Cycle Management Center
Hannah Easton, University of Dayton Research Institute
Andy Strat, Titan Robotics

5d. PROJECT NUMBER
WP-201709

5e. TASK NUMBER

5f. WORK UNIT NUMBER

7. PERFORMING ORGANIZATION NAME(S) AND ADDRESS(ES)
Air Force Life Cycle Management Center
n/a

8. PERFORMING ORGANIZATION REPORT NUMBER
WP-201709

9. SPONSORING/MONITORING AGENCY NAME(S) AND ADDRESS(ES)
Environmental Security Technology Certification Program
4800 Mark Center Drive, Suite 16F16
Alexandria, VA 22350-3605

10. SPONSOR/MONITOR'S ACRONYM(S)
ESTCP

11. SPONSOR/MONITOR'S REPORT NUMBER(S)
WP-201709

12. DISTRIBUTION/AVAILABILITY STATEMENT
DISTRIBUTION STATEMENT A. Approved for public release: distribution unlimited.

13. SUPPLEMENTARY NOTES

14. ABSTRACT
A robotic laser system was adopted at Hill Air Force Base, Utah, for use on the F-16 aircraft. The robotic laser system utilized 2010 technology with a 6 kW continuous-wave (CW) laser. Since that time, many advancements in technology have been accomplished within all critical areas specifically with the laser and sensors. The Air Force Life Cycle Management Center (AFLCMC) planned to develop and procure the next generation robotic laser coating removal system using the qualified 1 kW nano-pulse laser (NPF) for the Global Hawk and the C-130 aircraft at Robins Air Force Base, Georgia. The planned system would have incorporated advancements in laser scanners, surface mapping techniques, color sensors, and control technology.

The objective of the WP-201709 ESTCP Project was to validate and qualify a commercially available nano-pulsed 1 kW fiber laser system with a polygon scanner on thin advanced composites coated with traditional and non-traditional military paint colors, such as gloss white.

15. SUBJECT TERMS
Environmentally Preferred, Improved (Rapid) Laser Coating Removal Process, Safe Removal, Coatings, Composite Substrates

16. SECURITY CLASSIFICATION OF:			17. LIMITATION OF ABSTRACT	18. NUMBER OF PAGES	19a. NAME OF RESPONSIBLE PERSON
a. REPORT	b. ABSTRACT	c. THIS PAGE			Connor Eviston
UNCLASS	UNCLASS	UNCLASS	UNCLASS	81	19b. TELEPHONE NUMBER *(Include area code)* 937-255-7730 (administrative POC)

Contents

1.0 INTRODUCTION 2
1.1 BACKGROUND 2
1.2 DEMONSTRATION OBJECTIVE 2
1.3 REGULATORY DRIVERS 2
2.0 DEMONSTRATION TECHNOLOGY 4
3.0 PERFORMANCE OBJECTIVES 5
3.1 Flow Days 5
3.2 Substrate Integrity 5
3.3 Coating Removal 6
4.0 SITE/PLATFORM DESCRIPTION 7
4.1 Test Platforms/Facilities 7
4.1.1 Automotive and Industrial Supply Inc 7
4.1.2 Southwest Research Institute 7
4.1.3 Titan Robotics 7
4.1.4 University of Dayton Research Institute 8
4.2 Present Operations 9
4.3 Site-Related Permits And Regulations 10
5.0 TEST DESIGN 11
5.1 Open Loop Metallic Optimization Testing 11
5.1.1 Process Parameter Configuration 14
5.1.2 Materials 14
5.1.3 Panel Preparation and Coatings 16
5.1.4 Test Matrix/Testing Scenarios 18
5.2 Scanner Selection Testing 21
5.2.1 SCANLAB IntelliWELD (With beam shaping) 22
5.2.2 SCANLAB IntelliWELD (No beam shaping) 22
5.2.3 IPG Mid Power Scanner (Short Focal Length, 3mm spot size) 22
5.2.4 IPG Mid Power Scanner (Long Focal Length, 1.94mm spot size) 22
5.2.5 Important Laser / Scanner Parameter Definitions 22
5.3 Closed Loop Metallic Optimization 24
5.3.1 Panels 24
5.3.2 Coatings 25
5.3.3 De-Paint 25

5.4 Composite Optimization Testing 27
5.4.1 Materials 27
5.4.2 Panel Preparation and Coatings 32
5.5 Composite Screening Testing 34
5.5.1 Materials 34
5.5.2 Panel Preparation and Coatings 35
5.5.3 De-Paint 36
5.6 Demonstration 36
6.0 PERFORMANCE ASSESSMENT 37
6.1 Metallic Open Loop Optimization Testing 37
6.2 Scanner Selection Testing 37
6.3 Metallic Closed Loop Optimization Testing 38
6.3.1 Gray Topcoat 38
6.3.2 White Topcoat 38
6.3.3 Multi-Layer Gloss-White/Yellow Stackup 38
6.4 Composite Optimization Testing 39
6.4.1 Coating Removal Rate (ft^2-mils/min) 39
6.4.2 Maximum Temperature. 39
6.4.3 Visual Inspection. 39
6.5 Composite Screening Testing 45
6.5.1 Surface Roughness 47
6.5.2 Primer Adhesion 48
6.5.3 Cross-Section Visual Inspection 50
6.5.4 Long Beam Flexure 57
7.0 COST ASSESSMENT 61
7.1 Cost Model 61
7.2 Cost Analysis And Comparison 61
8.0 IMPLEMENTATION ISSUES 62
9.0 REFERENCES 63

Appendix A: Points of Contact
Appendix B: Ultimate Stress Graph
Appendix C: Chord Modulus Graph
Appendix D: Flexural Stiffness Graph

Figures and Tables

Figure 1	IPG 1 kW NPF Laser	page viii
Figure 2	Laser Enclosure	page 8
Figure 3	Laser Scanner Components and Mounting	page 12
Figure 4	Test panel position and transport	page 13
Figure 5	Thermocouple mounting	page 14
Figure 6	Panel Size and Layout	page 15
Figure 7	Panel Naming Convention	page 16
Figure 8	Custom Laser Enclosure	page 25
Figure 9	Panel Layout	page 27
Figure 10	Composite Panel Construction	page 28
Figure 11	Composite Optimization Test Panel Construction	page 31
Figure 12	M46J process side laminate skin with thermocouples embedded	page 32
Figure 13	Composite Screening Panel Layout and Cut Plan	page 36
Figure 14	Initial testing panels with embedded thermocouples	page 40
Figure 15	285 K Single Gray Stackup	page 41
Figure 16	M46J Single Gray Stackup	page 42
Figure 17	M46J Quad Gray Stackup	page 43
Figure 18	M46J White Stackup	page 44
Figure 19	M46J Single Gray with Surface Sealer Results	page 44
Figure 20	T650 Single Gray Stackup	page 45
Figure 21	Screening Test Results Visual Post De-paint	page 47
Figure 22	Surface Roughness Testing	page 48
Figure 23	Surface Roughness Imaging	page 48
Figure 24	Crosshatch Adhesion Testing Classification System	page 49
Figure 25	Pattie Adhesion Testing	page 50
Figure 26	Cross Section Locations of Control Panels	page 51
Figure 27	Cross Section Locations of Test Panels	page 52
Figure 28	Cross Section of 285 K Control	page 54
Figure 29	Cross Section of 285 K De-painted Panel	page 54
Figure 30	Cross Section of M46J Control Panel	page 54
Figure 31	Cross Section of M46J G NPF De-painted Panel	page 55
Figure 32	Cross Section of M46J S G NPF Control Panel	page 55
Figure 33	Cross Section of M46J GT NPF De-painted Panel	page 56
Figure 34	Cross Section of T650 Control Panel	page 56
Figure 35	Cross Section of T650 De-painted Panel	page 57
Figure 36	Four Point Long Beam Flexure Test	page 58

Table 1	Nominal Laser Operating Modes	page ix
Table 2	Summary of Composite Screening Test Results	page xii
Table 3	Performance Objectives	page 5
Table 4	Substrates and Initial Surface Treatments	page 15

Table 5	Test Matrix 1	page 20
Table 6	Test Matrix 2	page 21
Table 7	Scanner Parameters by Configuration	page 21
Table 8	Laser Spot Characteristics	page 23
Table 9	Aluminum Substrates and Initial Surface Treatments (sec 5.3.1)	page 24
Table 10	Laser Pulse Modes (sec 5.3.3.2)	page 26
Table 11	Composite Material Selection (sec 5.4.1.1)	page 27
Table 12	Composite Panel Skin Specification (5.4.1.2)	page 29
Table 13	Composite Panel Sandwich Specification (sec 5.4.1.2 – further)	page 30
Table 14	Panel Material Source Information (sec 5.4.1.3)	page 32
Table 15	Panel Preparation and Coating Summary (sec 5.4.2)	page 33
Table 16	Panel Preparation and Coating Information	page 35
Table 17	Trade-Off Comparison	page 37
Table 18	Area Coverage Rates by Scanner	page 37
Table 19	Selected IntelliWELD30 recipes (All panels 0.032" Bare Aluminum)	page 39
Table 20	Selected Laser Coating Removal Parameters for Composite Substrates	page 40
Table 21	285 K Single Gray Coating Results	page 40
Table 22	M46J Single Gray Coating Results	page 41
Table 23	M46J Quad Gray Coating Results	page 42
Table 24	M46J White Coating Results	page 43
Table 25	M46J Single Gray with Surface Sealer Results	page 44
Table 26	T650 Single Gray Results	page 45
Table 27	Composite Screening Material Property Test Results Summary	page 46
Table 28	Crosshatch Tape Adhesion Test Results	page 49
Table 29	Patti Adhesion Test Results	page 50
Table 30	Sandwich Construction and Corresponding Sample IDs	page 59
Table 31	Results Summary	page 59
Table 32	Statistical Analysis Results	page 60

ACRONYMS AND SYMBOLS

°C	degree(s) Celsius
°F	degree(s) Fahrenheit
ACT	Applied Corrosion Technologies
AIS	Automotive and Industrial Supply Inc.
AFLCMC	Air Force Life Cycle Management Center
AFMC	Air Force Materiel Command
AFOSH	Air Force Occupational Safety and Health
AFRL	Air Force Research Laboratory
ANSI	American National Standards Institute
ASTM	American Society for Testing and Materials
CAA	chromic acid anodizing
CAA	Clean Air Act
CWA	Clean Water Act
COTS	commercial-off-the-shelf
Cr	Chromium
CW	continuous wave
DoD	Department of Defense
E-coat	electrodeposition coating
EMI	electromagnetic interference
ESTCP	Environmental Security Technology Certification Program
EU	European Union
EZP	Product Support Engineering Division
GALVO	galvanometer
HAP	hazard air pollutants
HEPA	high-efficiency particulate air
HVAC	heating, ventilation, and air conditioning
HVLP	high volume low pressure
Hz	hertz
IAW	in accordance with
ICBM	Intercontinental Ballistic Missile
IPG	IPG Photonics Corporation
ISO	International Organization for Standardization
JTP	Joint Test Protocol
kHz	kilohertz
kW	kiloWatt
LCR	laser coating removal
m	meters
mils	thousandths of an inch
mJ	millijoule
MW	megawatt
M&S	maintenance & sustainment
nm	nanometer

NPF	nano-pulse laser
ns	nanosecond
OEM	original equipment manufacturer
OML	outer mold lines
OSHA	Occupational Safety and Health Act
PI	principal investigator
PMB	plastic media blast
PPE	personal protective equipment
PPG	Pittsburgh Plate Glass
PRR	pulse repetition rate
RCRA	Resource Conservation Recovery Act
R&D	research & development
RLCRS	Robotic Laser Coating Removal System
RoHS	restriction of hazardous substances
s	seconds
SAE	Society of Automotive Engineers
SBIR	small business innovative research
SwRI	Southwest Research Institute
um	micrometer
U.S.	United States
UDRI	University of Dayton Research Institute
USAF	United States Air Force
WR-ALC	Warner Robins Air Logistics Complex

ACKNOWLEDGEMENTS

First, we would like to thank ESTCP for the funding and opportunity to investigate the nanosecond (ns) pulsed laser technology.

We also wish to acknowledge the assistance of Mr. Randall Straw and Mr. Jesse Holdaway for their support early on and throughout the project.

Finally, we are grateful for the large role Ms. Natalia Voevodin played throughout the project and her expertise of the ESTCP processes.

ABSTRACT

Introduction and Objectives

A robotic laser system was adopted at Hill Air Force Base, Utah, for use on the F-16 aircraft. The robotic laser system utilized 2010 technology with a 6 kW continuous-wave (CW) laser. Since that time, many advancements in technology have been accomplished within all critical areas specifically with the laser and sensors. The Air Force Life Cycle Management Center (AFLCMC) planned to develop and procure the next generation robotic laser coating removal system using the qualified 1 kW nano-pulse laser (NPF) for the Global Hawk and the C-130 aircraft at Robins Air Force Base, Georgia. The planned system would have incorporated advancements in laser scanners, surface mapping techniques, color sensors, and control technology.

The objective of the WP-201709 ESTCP Project was to validate and qualify a commercially available nano-pulsed 1 kW fiber laser system with a polygon scanner on thin advanced composites coated with traditional and non-traditional military paint colors, such as gloss white.

Technology Description

Using an Air Force purchased commercial IPG 1 kW NPF laser with a Lincoln Polytek Polygon scanner, validation and qualification testing were accomplished. Pre-screening tests were accomplished using Global Hawk with generic composite and aluminum substrates; in conjunction with associated aircraft surface treatments, primers, and topcoats.

Tests utilized an IPG 1 kW nanosecond pulsed fiber (NPF) laser (**Figure 1** IPG 1 kW NPF Laser) with 1.06 um wavelength (IPG YLPN-100-30x100-1000). This laser provided a pulsed output with a maximum pulse energy of 100 mJ. The laser had four nominal operating modes with associated pulse duration, repetition rate, and energy (**Table 1** Nominal Laser Operating Modes**)**. All modes provided 1 kW averaged power output. Tests utilized the nominal operating modes.

Figure 1 IPG 1 kW NPF Laser

Table 1 Nominal Laser Operating Modes

Nominal Laser Operating Modes		
Pulse Duration	Pulse Rate	Pulse Energy
ns	kHz	mJ
30	20	50
40	13.3	75
60	10	100
100	10	100

Laser power was delivered to a scanner by a process fiber (fiber-optic cable) with a 600 um square fiber core and 20m length. The large core size and square cross-section of the process fiber yielded a square beam shape with a flat-top (uniform) intensity distribution on the work surface.

Performance and Cost Assessment

Nano-pulse fiber laser allowed the coating to be removed rapidly at higher peak energy levels. The laser beam moved faster over the surface and allowed for lower substrate temperatures, which is critical for composite materials as well as faster strip rates.

There was no cost-benefit analysis accomplished on this project.

Implementation Issues

A consistent issue with implementing this project was the change in scope. The proposal was for composite panel testing, which then changed to include metallic panels because they were cheaper and faster to purchase for the project. The testing included the use of a Lincoln Polytek Polygon scanner with the 1 kW NPF laser system. The Lincoln Polygon proved to be too large and cumbersome for use on the end effector and was ultimately replaced with a Galvanometer (GALVO) scanner.

Publications

There were no publications.

Security Review

An applicable security review was conducted to verify the applicable distribution statement.

EXECUTIVE SUMMARY

Introduction

Robotic laser coating removal was implemented at Hill Air Force Base using a 6 kW CW neodymium doped ytterbium arsenic garnet (Nd:YAG) laser. This has proven to drastically reduce the amount of hazardous waste generated by chemical and media blasting de-paint processes. While the 6 kW CW Nd:YAG laser effectively and efficiently removes the most common gray top coats and chromate yellow primers, the removal rate is drastically decreased for pale or gloss coatings. Additionally, the current Robotic Laser Coating Removal System (RLCRS) process required leaving 3 mil of coating over composite substrates to ensure damage is not caused to the resins or fibers. This testing was part of an ongoing investigation for alternate laser types that can effectively remove these additional coatings and remove down to the composite substrate. The 1 kW nanosecond pulsed fiber laser was initially promising.

Objectives

- Evaluate coating removal setting to optimize parameters for fastest coating removal while ensuring substrate integrity
- Develop integrated system with automated coating recognition and power suppression

Technology Description

The laser evaluated during this project was an Ytterbium Fiber Laser with a configurable pulse length of 30-100 ns utilizing a 600 um core fiber delivery system. This class 4 laser was produced by IPG Photonics and required a 3 phase, 60 Hz power supply and an external chiller. This laser was paired with multiple scanners throughout the project.

Performance Assessment

The performance of the 1 kW NPF laser for application as an alternate outer mold line RLCRS was conducted in four phases: metallic optimization, scanner selection, composite optimization, and composite screening. Each of these phases produced valuable results. However, it was concluded that although previously difficult coatings are removable with insignificant effect to the composite substrate, the 1 kW system does not provide a fast enough coating removal rate to justify progressing to implementation.

Metallic Optimization

Optimization was first conducted on metallic substrates to minimize the cost and lead time of beginning work. Optimization was conducted at Southwest Research Institute (SwRI) in San Antonio, Texas. Various power densities were investigated to determine the best removal rate while maintaining a backside substrate temperature under the F-16 flight service temperature of 300ºF. The results of this testing indicated that in order to achieve acceptable coating removal rates

and maintain a reasonable end effector unit for the RLCRS, alternative scanners should be considered.

Scanner Selection Testing

Scanner selection testing was conducted at Titan Robotics in which three scanners were evaluated for the application. The scanlab intelliWELD 30 was selected for the remainder of the testing.

Composite Optimization

The nano-pulse laser effectively removed the topcoat, while leaving the primer intact and did not affect the composite substrates. One significant advantage of the nano-pulse laser was the reduced thermal effects on the substrate. This occurred because the coating removal method used by the nano-pulse laser is ablation versus thermal decomposition, which was used by CW lasers.

Composite Screening

Screening tests using composite and aluminum panels validated that temperatures during processing only varied between 100°F and 140°F (peak). This was dependent upon panel thickness, coating color, and thermocouple location on the panels. Additionally, the primer layer was not removed which ensured that the laser energy was never directly applied to composite fibers and resins. Primer adhesion results showed no degradation of the primer. However, initial mechanical tests showed a high likelihood that no damage to the composite substrate was caused by the laser de-paint process. Ultimately these tests were found to be inconclusive. Results are summarized in **Table 2**.

Table 2 Summary of Composite Screening Test Results

Panel ID	Num passes	Surface Roughness (Average)	Patti Adhesion (average pull off psig)	Crosshatch Tape Adhesion (Pass: Fail)	Cross Section	Long Beam Flexure (stat. Diff. From control)
M46J_0_0_G_NPF_01	13	2.852	19.2	3:5	Minor surface damage	bottom face sheet effective chord modulus only
M46J_0_S_G_NPF_01	15	3.196	34.1	8:0	No damage	No statistical difference
M46J_0_0_GT_NPF_01	>40	5.597	20.7	7:1	damage	Flexural stiffness only
M46J_0_0_W_NPF_01	not processed; optimized parameters not found by project halt					
M46J_0_0_0_CTL_CTL	N/A	1.834	19.0	0:8	-	-
285K_0_0_G_NPF_01	7	2.368	22.6	8:0	damage	Multiple
285K_0_0_0_CTL_CTL	N/A	1.901	10.6	2:6	-	-
T650_0_0_G_NPF_01	12	2.922	16.3	8:0	damage	Bottom face sheet ultimate stress only
T650_0_0_0_CTL_CTL	N/A	0.829	15.8	3:5	-	-

Cost Assessment

The desired application for this technology was deemed inefficient prior to conducting cost-benefit analysis.

Implementation Issues

Implementation nor demonstration were performed as the removal rate of the current continuous wave RLCRS is superior to what was achieved using the 1 kW nanosecond pulsed fiber laser.

1.0 INTRODUCTION

1.1 Background

The ESTCP WP-201709 project supported efforts of the AFLCMC/EZP mission for sustainment of a wide range of United States Air Force (USAF) weapon systems. This specifically included the management of corrosion on aircraft structures, which required periodic coating removal and replacement. For several decades, the USAF has invested in development and qualification of new processes for coating removal, including plastic media blasting (PMB) and laser coating removal (LCR).

Progress in the scale-up and commercialization of LCR made it economically attractive for full airframe application. Airworthiness certification of LCR processes required to support its adoption. This project supported a program for certification of NPF laser systems on multiple airframes.

Traditional aircraft coating removal methods, such as: chemical stripping, PMB, and hand sanding generate excessive costs. These costs are associated with: materials handling, waste removal, personal protective equipment (PPE), emission tracking and reporting, and labor. AFLCMC/EZP was focused on redefining the traditional aircraft coating removal process and replacing it with laser technology in a variety of applications. These applications include: full-aircraft coating removal, off-aircraft components coating removal, confined space coating removal, and coating removal using a hand-held laser. This project supported AFLCMC/EZP efforts to qualify the use of 1 kW NPF laser with a robotic arm for aircraft coating removal on composite substrates.

Laser coating removal has been successfully demonstrated on metallic substrates on the F-16 and the C-130 aircraft. It is an alternative to the current environmentally burdensome coating removal methods of hand sanding, wheat starch blasting, and chemical stripping from composite aircraft. Those processes generate large volumes of hazardous waste, expose workers to hazardous environments and cause severe ergonomic harm to workers. This is in addition to the significant costs involved. The hypothesis was that the 1 kW nano-pulse would generate small amounts of hazardous waste and impart minimal damage to the substrate on composite materials.

1.2 Demonstration Objective

The demonstration plan was not achieved. The project was stopped by ESTCP at the point where the demonstration plan was initiated.

1.3 Regulatory Drivers

Large quantities of hazardous waste are commonly generated by DoD depot-related activities. The wastes that are associated with coatings removal include: the disposal of liquid paint removers; contaminated rinse water, from chemical stripping operations; and media waste, resulting from a variety of blasting processes.

Coatings removal activities are impacted by several regulations promulgated under the Clean Water Act (CWA), Clean Air Act (CAA), and Resource Conservation and Recovery Act

(RCRA). Washing surfaces following de-painting operations can generate quantities of wastewater contaminated with methylene chloride or media and paint residue. Discharging wastewater with traces of hazardous waste can result in a direct violation of the CWA. The most common regulation associated with de-painting activities is the CAA, including the recent efforts to minimize the use of Hazard Air Pollutants (HAP) such as methylene chloride. The RCRA directly regulates disposal of wastes generated by de-painting activities. The RCRA regulates how and where de-painting waste can be disposed and transported as well as any future liabilities resulting from environmental damage.

Chemical and mechanical coatings removal operations also require consideration for worker protection and training under the Occupational Safety and Health Act (OSHA), Air Force Occupational Safety and Health (AFOSH) standard, or other service specific occupational safety and health directives as appropriate. In the event where these standards overlap the more stringent standard is to be followed.

2.0 DEMONSTRATION TECHNOLOGY

The laser evaluated in this testing was an IPG 1 kW nano-pulsed laser operating at 1064 nm wavelength and with 4 pulse durations of 30, 40, 60 and 100 nanoseconds (ns). The pulse energies varied from 50 to 100 millijoules (mJ). Selectable pulse repetition rates varied from 2 to 50 kilohertz (kHz). The laser fiber delivery from the laser generator was a 600 micron (side length) square fiber with a roughly uniform intensity profile. No demonstration of the evaluated technology occurred.

3.0 PERFORMANCE OBJECTIVES

Laser coating removal is being considered by the Air Force for use on military assets in an effort to provide safer working conditions for operating personnel while reducing environmental impacts. The system at Hill Air Force Base, Utah met challenges with pale / gloss coatings, as well as, requirements to leave coating over composite surfaces. Each of the performance objectives shown in **Table 3** was designed to evaluate feasibility and seamless transition for the maintenance staff to use on the C-130 at Robins Air Force Base, Georgia.

Table 3 Performance Objectives

Performance Objective	Data Requirements	Success Criteria	Results
Quantitative Performance Objectives			
Decreased Flow Days Coating removal rate	• Volumetric estimate	Reduction from current 6 kW process	Fair
Low Impact on Substrate Laboratory testing	• ASTM and SAE type tests (see below)	No Change from baseline as described in JTP (Appendix A)	Inconclusive; changes occurred, causes unknown
Qualitative Performance Objectives			
Increased Applicability Visual inspection	• Visual inspection	Removal of White coatings, removal over composite substrates	Success
Minimized Post Processing Visual Surface Finish	• Feedback from field technician on preparation for recoating	Minimal sanding required	Demonstration not Performed

3.1 Flow Days

Flow days are an important criterion for a successful transition. To ensure there was no interruption, matching the current flow days was required for the entire de-paint / re-paint process, with the overall desire to reduce the flow days. The current 6 kW laser coating removal system, was considered to provide a comparable flow days estimate in comparison to the plastic media blast method for the F-16 aircraft at Hill Air Force Base.
When considered on a "surface area per time" basis, the chemical striping used on the C-130 was drastically faster. Laboratory scale coating removal rate was calculated based on: average coating thickness, laser on time, laser power, and test area size. This was expressed in ft^2 mils / kW min. This value could be extrapolated to estimate the flow days required to laser de-paint the C-130.

3.2 Substrate Integrity

The technology is not practical if the integrity of the aircraft substrate is compromised, even if the time performance basis were compatible. Substrates were evaluated through laboratory testing as follows:

Aluminum Substrates:

- Substrate temperature
- Visual inspection
- Adhesion testing (ASTM D3359)
- Surface metallography (ASTM E7)

- Cross section analysis (ASTM E3)
- Rockwell hardness (ASTM E18)
- Electrical conductivity (MIL-STD-1537)
- Residual stress (SAE J-442)
- Tensile testing (ASTM E8)
- Fatigue (ASTM E466)

Composite Substrates:

- Substrate temperature
- Visual inspection
- Adhesion testing (ASTM D3359)
- Surface roughness (ASTM D7127)
- Long beam flexure (SAE MA4872 and ASTM D7249)

These tests and results are described in full detail in Sections 5.0 and 6.0.

3.3 Coating Removal

The technology must be capable of effectively removing the gloss white coating and cleanly removing all coatings down to the composite surfaces on the C-130 airframe, which was difficult for the current 6 kW Hill RLCRS. Extending coating and substrate applicability will also allow the potential for additional airframes. Laboratory testing on panels were conducted to include gloss white coating and composite substrates. Qualitative observation was the main evaluation process as to capability, with later coating removal rate calculation guiding system parameter selections.

Minimization of post processing was an important factor in transition of the laser coating removal into the depot system. A qualitative visual inspection was performed to verify damage has not occurred and surface can easily be recoated.

4.0 SITE/PLATFORM DESCRIPTION

4.1 Test Platforms/Facilities

4.1.1 Automotive and Industrial Supply Inc.

Automotive and Industrial Supply Inc. (AIS) is a small business established in 1996 that operates out of four locations. Coating application was performed at the main location in Ogden, Utah. AIS was able to source the necessary aerospace coatings, as well as, apply and conduct adhesion and coating thickness testing to ensure proper application.

4.1.2 Southwest Research Institute

Southwest Research Institute in San Antonio, Texas, conducted some initial optimization work using the IPG 1 kW NPF laser with 1.06 um wavelength (IPG YLPN-100-30x100-1000). The laser was set up in conjunction with a 20 kW CO2 laser and utilized the same non-laser-specific lab hardware. This laser provided a pulsed output with a maximum energy of 100 mJ. Nominal pulse duration was 60 ns at a pulse rate of 10 kHz, but these were configurable. Laser power was delivered from the source to the work by a fiber-optic cable, lenses, and mirrors. The fiber-optic cable had a square cross-section and produced a square beam profile with a flat-top (uniform) intensity distribution on the work.

Beam scanning (1D) on test panels was provided by a Lincoln Laser POLYtek polygon scanner. Scan width was approximately 56 mm. Scan velocity was nominally 2.7 m/s and was configurable. Laser spot size is nominally 1.3 mm square but was adjustable via a beam expander. Test panels were translated beneath the laser swath by a linear motion system.

The laser was transmitted approximately five inches from the output scan lens to the work surface. Process effluent was collected by an intake nozzle near the laser swath and routed to a HEPA filter system. Test panels were translated beneath the laser swath by a linear motion system. Nominal sweep rate (panel velocity) was approximately 20 mm/s but was configurable.

4.1.3 Titan Robotics

Titan established within its facility a laser lab in support of the 1 kW NPF laser testing and development. This included required laser safety measures, HVAC, electrical, and facility modifications. The lab also included a self-contained enclosed linear-axis table to do initial testing and integration. Specifically included in the laser test cell and standalone enclosure were:

- 3D scanner intrinsic functions for focus, scan speed, and scan width parameter exploration
- Control software for IPG 1 kW NPF fiber laser pulse properties (i.e. duration and rate)
- Commercial-off-the-shelf (COTS) linear axis for sweep speeds up to 200 mm/s
- Mechanical repositioning possible for working distance adjustment if needed
- Self-contained environmental cell with the Yaskawa MH-80 arm and end effector installed to provide an advanced optimization testing capability

All testing was performed in a custom laser safe enclosure measuring roughly 8x4x4 feet, as shown in **Figure 2**. The laser scanners are swappable, and mounted in the center aiming down at a fixture for test panels riding on a linear rail capable of moving at speeds up to 200 mm/s.

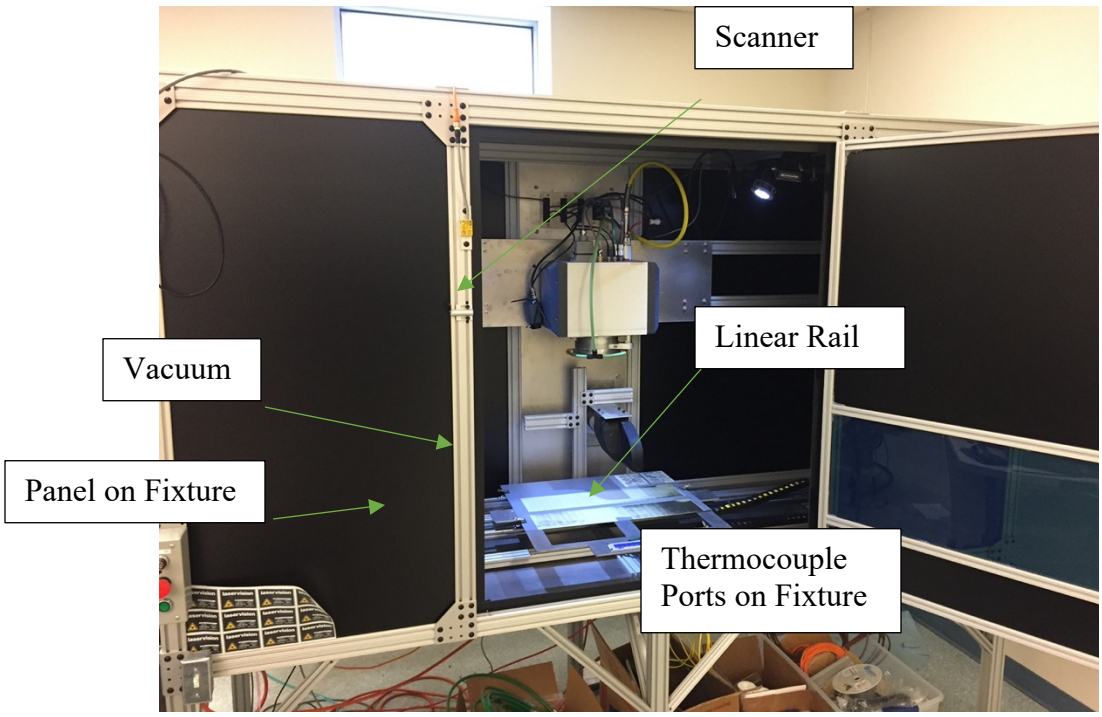

Figure 2 Laser Enclosure

4.1.3.1 Air Handling

Laser coating removal inherently creates hot high velocity particulate during processing. It is therefore important to manage the air between the scanner and the surface to collect the effluent, protect the equipment, and prevent shadowing of the surface (which leads to diminished performance).

To accomplish this, a vacuum nozzle was mounted above the surface just to the side of the laser processing point. This vacuum nozzle was ducted externally to a Teka FilterCube via hard ducting with a pressure relief valve so that flow rate was adjustable.

4.1.4 University of Dayton Research Institute (UDRI)

Material properties testing was conducted at some of UDRI's many test laboratories located in Dayton, Ohio. Each laboratory used is described in the following subsections.

4.1.4.1 Applied Corrosion Technologies Laboratory

The Applied Corrosion Technologies (ACT) Group conducted adhesion and surface roughness testing. The lab focused on: environmentally desirable coating removal processes; better understanding asset condition, based on cumulative exposure; and promoting the use of mission- and cost-effective alternative coatings and application processes. This supports the Air Force for use in transitioning to new technology. ACT provides subject matter expertise in cradle-to-grave

corrosion prevention and control of legacy and emerging systems. This group has the facilities, equipment, and capability for:

- Salt fog, UV exposure, temp, and humidity etc.
- Plastic media and steel shot blast
- Laser de-paint of material
- Coating adhesion testing
- Outdoor exposure
- Paint application (HVLP spray booth)
- Powder coat application
- Quick screening laboratory
- E-coat (Electrodeposition coating)
- Metal sheering and mechanical engraving

4.1.4.2 Composites Manufacturing and Testing Laboratory

Four-point long beam flexure testing was conducted by the Multifunctional Structures and Materials Group. In this laboratory, researchers conduct research & development (R&D) programs involving a wide range of adhesive, composite, plastic, and core materials. They process and evaluate fiber-reinforced polymeric composite materials, adhesives and primers, cores, fabrics and textiles, and transparency and plastic materials. The laboratory is an International Organization for Standardization (ISO) 9001:2015 registered Composites Manufacturing and Testing laboratory. This laboratory contains a wide array of equipment for processing, as well as evaluating adhesives, primer, fiber-reinforced polymer matrix composites, nanocomposites, and plastic materials used in military and commercial applications. In the laboratory, researchers perform both routine and specialized evaluations and material characterizations on composites, adhesives, sandwich constructions, and plastics. The laboratory is fully equipped to process and machine all types of fiber-reinforced composite and bonded adhesive joint test coupons. The laboratory has the following capabilities:

- Composites manufacturing
- Composites testing
- Additive manufacturing
- Autoclave capabilities
- Electromagnetic interference (EMI) shielding
- Environmental conditioning
- Adhesive bonding technology
- Nanocomposite coating

4.2 Present Operations

The qualified 6 kW CW laser utilizes combustion and pyrolysis of the coatings as the means for removal. This process is relatively slow when compared to an ablation process used by nano-pulse lasers. Ablation imparts magnitudes of higher energy at a much quicker rate, which then causes the coating to explode and turn into plasma since it cannot transfer the energy quickly enough. During the much slower pyrolysis process, the polymeric portion of the coating is combusted and vaporized. This results in a flame emanating from the surface being lased with much of the laser

energy being transmitted to the substrate. In addition, a large flame is generated which imparts additional thermal energy to the substrate. Nano-pulse fiber lasers use a different mechanism for coating removal than CW lasers. Nano-pulse lasers utilize the ablation process that imparts high peak energy per pulse but for very short durations. This energy strikes the coating with a short duration pulse, which minimizes energy transfer to the substrate. This results in plasma formation and elimination of the coating at very high rates. This ablation process imparts significantly less energy into the substrate since the laser energy is absorbed into the coating and not into the substrate. Since the coating is removed rapidly at higher peak energy levels, the laser beam moves faster over the surface and allows for lower substrate temperatures. This is critical for composite materials, as well as, faster strip rates.

4.3 Site-Related Permits and Regulations

No site-related permits were required for the demonstration, as it did not take place. No regulations were impacted because the demonstration did not take place.

5.0 TEST DESIGN

Previous testing was conducted using the IPG laser at IPG laboratory in 2016, prior to the effort funded under ESTCP. Results of that testing indicated that the 1 kW laser is capable and viable of removing coatings while leaving substrates intact. However, the investigation of superior scanning technology is necessary to implement the full capabilities of the laser for de-paint purposes. As such, testing was designed in a phased approach with each phase outlined in the following subsections. Testing on metallic was performed prior to evaluating effects on composite substrates due to the cost and lead time associated with composites in comparison.

5.1 Open Loop Metallic Optimization Testing

Initial optimization testing was conducted at SwRI in San Antonio, Texas. 0.032" aluminum substrates were used with the goal of determining optimized process parameters.

Tests used a configurable laser scanner (**Figure 3** Laser Scanner Components and Mounting) providing a range of spot sizes and scan velocities. Brackets cantilevered from a rigid support structure supported the scanner assembly over a linear rail providing test article transport. The process fiber was mated to a collimator with 60 mm focal length (IPG P30-001214). Collimated beam size was adjusted via a zoom beam expander (Sill Optics S6EXZ5312-328). This was mounted in reverse to provide a range of spot sizes (1.4 – 2.8 mm). Beam scanning (1D) was provided by a Lincoln Laser POLYtek polygon scanner. A 100.3 mm focal length scan lens (Sill Optics S4LFT4010-328) provided a maximum scan width of 49.5 mm. The scanner was specially configured to support low scan velocities (to approximately 2.7 m/s). Tests were conducted at scan velocities ranging from 4.5 to 19 m/s.

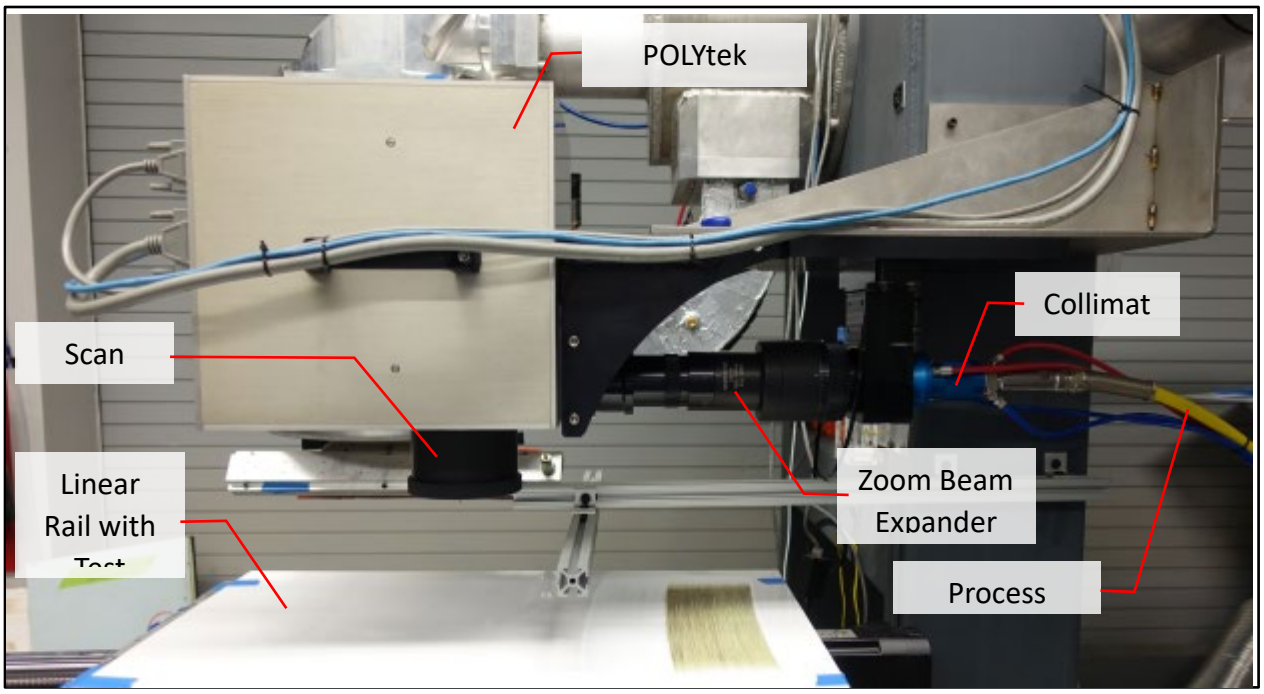

Figure 3 Laser Scanner Components and Mounting

The scan lens provided a working distance of 130 mm. The test panel position and transport is depicted in **Figure 4**. A screw-drive linear motion system provided test panel transport at speeds (sweep velocity) ranging from 17 to 145 mm/s. An extraction nozzle positioned near the scan line conveyed process effluent to a HEPA filter system.

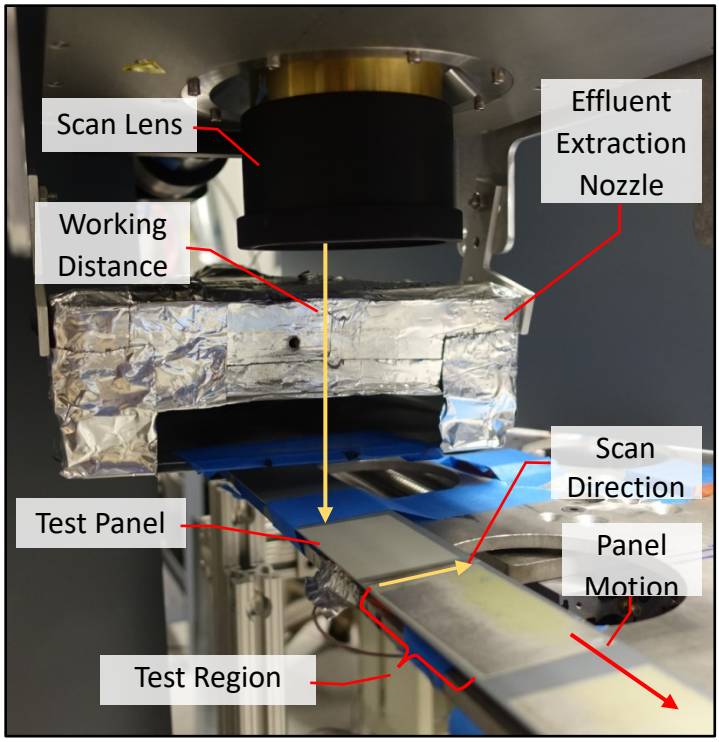

Figure 4 Test Panel Position and Transport

Substrate temperature was measured (at 10 Hz) using two fast-response self-adhesive T-type thermocouples (Omega Engineering PN SA1XL-T-72-SRTC) attached to the panel bottom side as depicted in **Figure 5**. Insulating supports were used to reduce heat transfer to the linear rail support plate. Optimization tests were conducted on sub-panels cut from parent panels (**Figure 5**) to further reduce heat transfer. Sub-panel width was slightly greater than the laser scan line length.

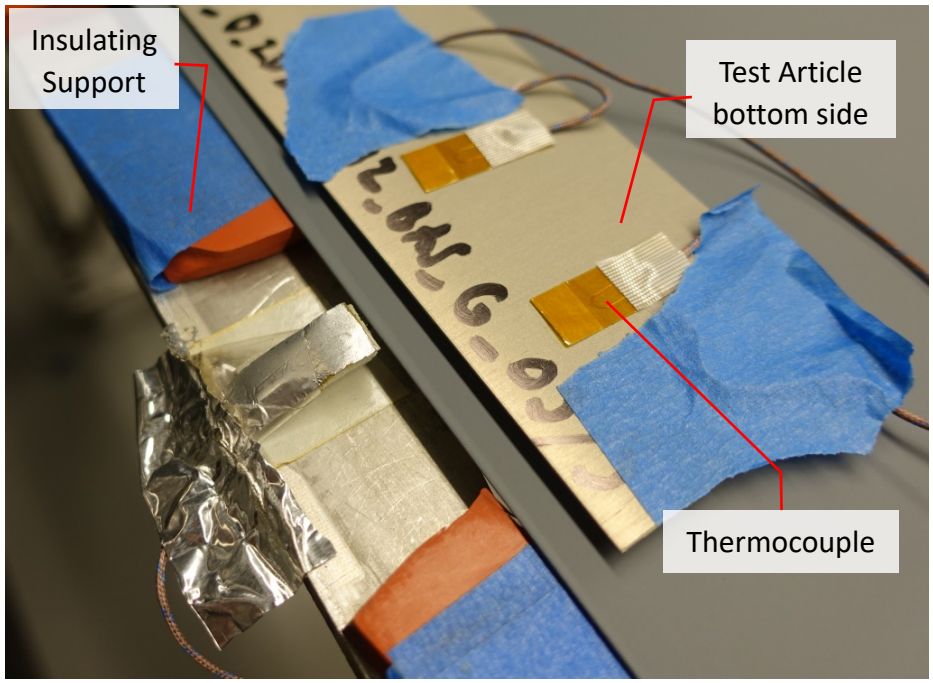

Figure 5 Thermocouple Mounting

5.1.1 Process Parameter Configuration

The following procedure was used to configure process parameters on the test system:

1. Laser pulse duration was set on the IPG laser through a serial interface. This also selected the nominal pulse repetition rate and pulse energy settings.
2. Spot size was set by adjusting the magnification of the zoom beam expander, with reference to a calibration between spot size and magnification.
3. Polygon speed was calculated from spot size, spot step, and pulse rate. Polygon speed was set on the polygon motor speed controller through an Ethernet interface. Polygon speed was also used to calculate a time delay, which was set on the POLYtek scan controller to synchronize laser scan line emission with polygon rotation angle.
4. Sweep velocity (linear rail) was calculated from the spot size, scan rate (from polygon speed), and scan step. Sweep velocity was set on the linear rail motion controller.

5.1.2 Materials

Materials used in the test report are summarized in the following sub-sections.

5.1.2.1 Substrates

Substrates were 2024-T3 bare and clad aluminum. Only 0.032" thickness substrate was tested. Substrates received initial surface treatments listed in **Table 4.**

Table 4 Substrates and Initial Surface Treatments

Aluminum Substrates and Initial Surface Treatments			
Substrate ID[1]	Material	Thickness (inch)	Initial Surface Treatment
2024_032_BN	2024-T3	0.032	None
2024_032_BA	2024-T3	0.032	Anodize - MIL-A-8625, Type I, Class 1
2024_032_CC	2024-T3 Clad	0.032	CCC - MIL-DTL-5541, Class 1, Type 1A
1. Last field of ID: BN (bare, no treatment), BA (bare, Anodized), CC (clad, chromate conversion)			

5.1.2.2 Panel Size and Layout

Panel size and layout are illustrated in **Figure 6**. Panel ID was marked on the back side of each panel. The ID was marked on each sub-panel after sub-panels were cut. The panel ID naming convention is shown in **Figure 7.**

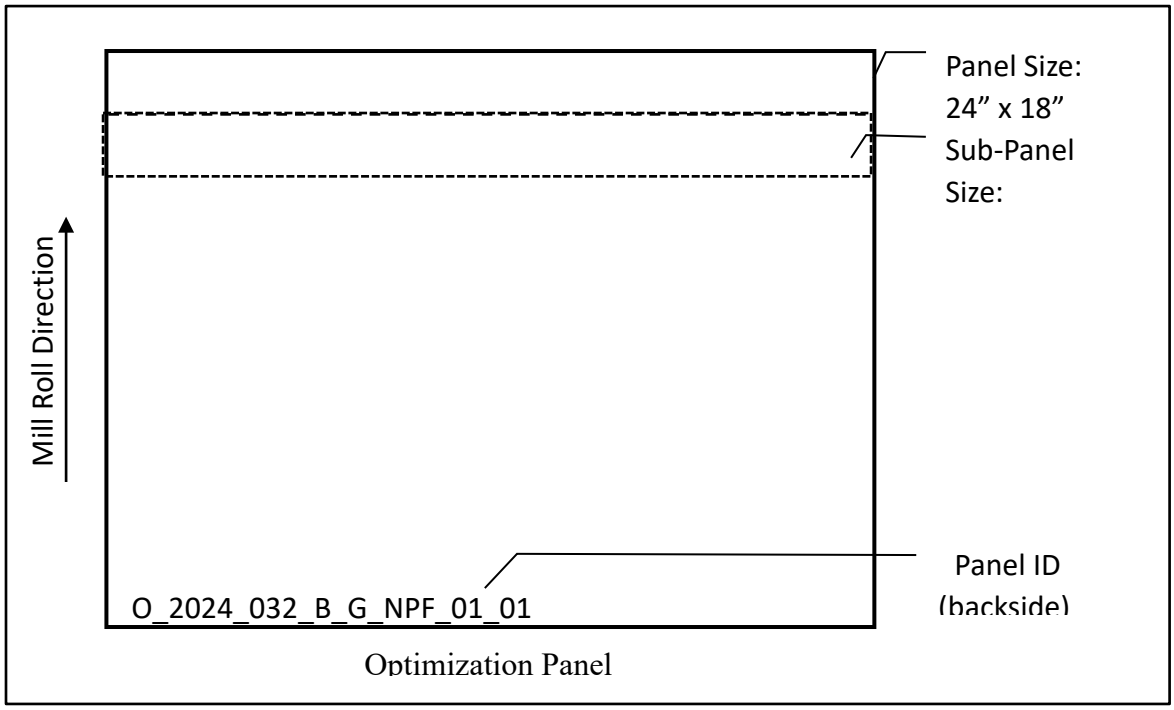

Figure 6 Panel Size and Layout

Panel ID Naming Convention
O_2024_032_BN_G_NPF_PN_SP Sub-Panel Number Panel Serial Number LCR Treatment[3] Coating Color & Thickness[2] Substrate & Pretreatment[1] Thickness (Thousandths of inch) Alloy & Temper (2024-T3) Optimization Test Panel
1. Substrate & Pretreatment: Bare-None (BN), Bare-Anodized (BA), Bare-Anodized-Sanded (BAS), Clad-Chromate_Conversion (CC) 2. Coating Color/Thickness: Gray noninal thickness (G), no coating (0) 3. LCR Treatment: Nano Pulsed Fiber (NPF), Control (CTL)

Figure 7 Panel Naming Convention

5.1.2.3 Procurement

Procurement details include:

1. Both bare and clad aluminum sheet was purchased from ThyssenKrupp Materials NA Inc.
2. The material suppliers cut the sheet stock into 18" x 24" panels with 18" dimension parallel to the mill roll direction.
3. Pre-Treatments (Anodize and Chromate Conversion) were both by Hohman Plating and Manufacturing out of Dayton, Ohio.
    a. Anodize pre-treatment was applied in accordance with (IAW) MIL-A-8625, Type I, Class 1.
    b. Chromate Conversion (alodine) pre-treatment was applied IAW MIL-C-5541, Class 1A.

5.1.3 Panel Preparation and Coatings

5.1.3.1 Anodized Sanded Treatment

Selected anodized panels were sanded to remove the anodized surface from the front (test) surface. The intent of this treatment is to be representative of airframes that have been previously subjected to mechanical coating removal cycles. In addition, this treatment has previously provided a reduced within-treatment variability of fatigue test results (relative to a bare alloy substrate). This supports greater sensitivity for detection of an LCR process effect.

The anodized coating was removed using a random orbital sander with a fine-grade Scotch-Brite™ aluminum oxide surface conditioning disc. This process is specific to primer removal from an anodized substrate (T0 1-1-8 Section 2.10.4), which provides the least possibility of substrate

damage. The removal process was applied until a bright, reflective aluminum base substrate started to become apparent through the matt anodized surface.

5.1.3.2 PreKote®

The sanded anodized panels received PreKote® surface pretreatment prior to the coating application as follows:

1. PreKote® was applied by SwRI.
2. PreKote® application was IAW TO 1-1-8 (180 grit aluminum oxide pad: A-A-58054, Type 1, Grade B) and the manufacturer instructions
3. Primer application commenced within 24 hours of PreKote® treatment

5.1.3.3 Primer

Military standard primer was applied as follows:

1. Primer was applied by SwRI
2. MIL-PRF-23377, Type I, Class C2 was used; specifically, PPG Desoprime CA7233
3. Primer application was IAW TO 1-1-8 and the manufacturer instructions
4. Application was to a DFT of 0.6 – 0.9 mils
5. Top coat application commenced no sooner than 5 hours and within 24 hours of primer application

5.1.3.4 Top Coat

Military standard top coat (production top coat for the C-130 and the RQ-4) was utilized, as follows:

1. Topcoat was applied by SwRI
2. MIL-PRF-85285, Type IV, Class H was used; specifically, PPG CA9311, color 36173 (gray)
3. Application was IAW TO 1-1-8 and the manufacturer instructions
4. Top coat was applied in three coats to a DFT of approximately 5 mils, with the total coating thickness (primer plus top coat) resulting in approximately 6 mils
5. A flash off time of 30 – 60 minutes between coats was provided

5.1.3.5 Accelerated Cure

An accelerated cure procedure (per test plan) was applied after the top coat application was completed. Both painted and unpainted control panels received the following curing procedure:

1. Painted panels dried for at least 60 minutes before starting the cure cycle
2. Painted panels were held at a minimum of 16 hours @ 145°F +/- 5°F in a drying booth

5.1.3.6 Sub-Panels

Sub-panels (24" x 2") were cut by a shear from parent panels after coating application and accelerated cure. Sub-panels were utilized to reduce heat transfer, relative to that anticipated from full-size panels, to improve the accuracy and repeatability of substrate temperature measurements.

5.1.4 Test Matrix/Testing Scenarios

5.1.4.1 Laser Process Parameters

Laser process parameters are defined in this section. Only a few parameters, as indicated below, were varied during optimization testing. Other parameters were held constant or were dependent on other parameters. Parameter values (including the recommended values for optimized parameters) are listed in **Tables 5 and 6.**

Tested/varied process parameters:

1. Pulse Duration – The duration over which the laser emits a pulse of light. Pulse durations associated with four nominal operational modes of the laser source were used (30, 40, 60, and 100 ns). See **Table 1** Nominal Laser Operating Modes
2. Spot Size – The dimensions of the focused beam on the coating/substrate. A single dimension (size) was provided since the beam shape was square.
3. Spot Step – The distance the beam moved between pulses as a percentage of the beam size. Spot step was selected as the reciprocal of an integer value (1/2, 1/3) to obtain uniform laser power application (scan fluence).
4. Scan Step – The distance the scan line moved between scan as a percentage of the beam size. Scan step was selected as the reciprocal of an integer value to obtain uniform laser power application (pass fluence).

Dependent or constant process parameters:

1. Wavelength – The peak emission wavelength of the laser.
2. Pulse rate – The frequency at which laser pulses repeat. The pulse rate corresponding to the selected pulse duration (nominal laser operational mode) was used, as depicted in **Table 1**.
3. Pulse energy – The energy in a single pulse. The pulse energy corresponding to the selected pulse duration (nominal laser operational mode) was used (**Table 1)**.
4. Output power – The time-averaged output power of the laser. The full rated output power of 1 kW was used for all tests. For each nominal operational mode, the product of pulse energy and pulse rate yielded an average power of approximately 1 kW.
5. Beam shape – The NPF laser had a square beam shape.
6. Beam profile – The NPF laser had flat-top beam intensity distribution.
7. Scan width – The length of the scan line was 49.5 mm. Scan width was a scanner design attribute.

8. Scan duty cycle – The (maximum) percentage of time over which the laser can traverse the scan line (40%). This was a scanner design attribute that impacts dependent process parameters.
9. Beam area – The surface area covered by the laser spot.
10. Pulse power – The average power imparted to the surface during each laser pulse.
11. Pulse intensity – The average power per unit area imparted to the surface during each laser pulse.
12. Scan velocity – The velocity of the laser spot along the scan line (spot size x spot step x pulse rate).
13. Scan frequency – The frequency (Hz) at which the scanned beam crossed a point on the scan line (scan velocity x scan duty cycle / scan width).
14. Sweep velocity – The velocity of scanner (or test panel) motion perpendicular to the scan line (spot size x scan step x scan frequency).
15. Time between passes – The minimum time between repeated passes (sweep direction). This period allowed the substrate to cool sufficiently to ensure that the allowable temperature did not exceed during repeated passes.
16. Working distance – The distance from a reference location on the scanner (e.g., output aperture) to the coating/substrate surface (130 mm, **Figure 4**. This was a scanner design attribute.
17. Scan fluence – The energy per unit area imparted during one scan of the laser spot (pulse energy / (spot size)^2 / spot step).
18. Pass fluence – The energy per unit area imparted during one pass of the scanner (scan fluence / scan step).

5.1.4.2 Bare Substrate Tests

Initial tests were conducted on a bare substrate processed with nominal high-fluence parameters to confirm that an acceptable substrate temperature (< 250 ºF) was achieved before proceeding with LCR tests. The 2024_032_BA (anodized) substrate was initially tested because this pre-treatment should have the greatest heating (greatest laser power absorption), based on prior experience. Subsequent bare substrate tests on 2024_032_BN (bare alloy) and 2024_032_CC (clad, conversion coating) were conducted to document the substrate/pretreatment effect on temperature. High fluence, for the purpose of this test, was achieved using a 33% spot step, 33% scan step, and high pulse energy (100 mJ).

5.1.4.3 LCR Parameter Optimization Tests

Initial parameter optimization tests measured LCR efficiency and substrate temperatures at the four nominal laser operating modes: pulse duration, with associated pulse rate, and pulse energy; and at three combinations of pulse step and scan step.

Table 5 Matrix 1

Test Matrix 1							
Group	Pulse Duration	Pulse Rate	Pulse Energy	Spot Step	Scan Step	Relative Scan Fluence	Relative Pass Fluence
	ns	kHz	mJ	%	%	%	%
A	100	10	100	50	50	100	100
				50	33	100	150
				33	33	150	225
B	60	10	100	50	50	100	100
				50	33	100	150
				33	33	150	225
C	40	13.3	75	50	50	75	75
				50	33	75	113
				33	33	113	169
D	30	20	50	50	50	50	50
				50	33	50	75
				33	33	75	113
E	30	20	50	25	50	100	100
				25	33	100	150

Table 6 Matrix 2

Spot Size	Pulse Duration	Pulse Rate	Pulse Energy	Spot Step	Scan Step	Relative Scan Fluence	Relative Pass Fluence
mm	ns	kHz	mJ	%	%	%	%
1.6	60	10	100	50	50	100	100
2.0	60	10	100	33	50	97	97
				50	33	64	97
2.3	60	10	100	25	50	97	97
				50	25	48	97
1.4	60	10	100	50	50	131	131
				33	33	198	300

The test matrixes, in **Tables 5 and 6**, provided a range of fluence levels resulting from the three pulse energies and spot/step combinations. Tested fluence levels ranged from 50% to 225% relative to the fluence obtained at the maximum pulse energy (100 mJ) with 50% spot and scan steps. Test Matrix 1 facilitated comparison of the 100 and 60 ns pulse durations which had the same pulse energy, and thus equivalent fluence levels. Test group E utilized a 25% spot step with the 30 ns pulse duration (50 mJ pulse energy) to obtain fluence levels comparable to 100 and 60 ns pulses (Groups A and B). Test matrix 1 was executed using 1.6 mm spot size.

5.2 Scanner Selection Testing

Titan Robotics Inc. evaluated two different models of galvanometer scanners, each in two configurations (four scanner configurations total) identified by UDRI and the Air Force as shown in **Table 7.** These scanners provided peak irradiances between 8.5 and 35 MW/cm^2. This set of configurations was chosen to allow for the parameter set to cover a wide variety of spot sizes and spot speeds. Scanner parameters that were inherent within each of the scanner designs were used for this program. Note that removing the beam shaping optic for the intelliWELD scanner made the spot height smaller.

Table 7 Scanner Parameters by Configuration

Scanner ID	intelliWELD with beam shaping	IPG Mid Power	IPG Mid Power	intelliWELD no beam shaping
Focal Length (mm)	460	254	163	460
Field Width (mm)	330	160	80	330
Max Spot Speed(m/s)	9	2.5	1.25	9
Focus Range(mm)	+/- 70	N/A	N/A	+/- 70
Spot Width(mm)	2.49*	3.03	1.94	2.49
Spot Area (cm^2)	*	0.0915	0.0377	0.062
Beam clipped (%)	8.9	22.2	22.2	8.9

5.2.1 SCANLAB IntelliWELD (with beam shaping)

The first scanner tested was a 460 mm focal length SCANLAB IntelliWELD. This scanner is controlled by an optical interface via the RTC4 card. It has a beam shaping optic installed, which was originally designed for a round fiber continuous wave laser system. The beam shaping optic is a cylindrical lens located just prior to the galvanometer mirrors. This optic elongates one axis of the spot, which creates an ellipse in the round fiber case or a rectangle for square fibers. This shaping occurs by defocusing the axis being elongated, for the pulsed laser, which causes the sharpness of the edge to blur and the uniformity of the intensity to degrade.

5.2.2 SCANLAB IntelliWELD (no beam shaping)

A second, but identical RTC4 controlled IntelliWELD 30 was tested with the exception that the beam shaping optic from this scanner was removed by Titan personnel to achieve a uniform energy distribution on the surface. The laser fiber bayonet adapter (and beam shaping optic) was installed by the manufacturer with a 30 degree or so twist. This resulted in rotated spots on the surface, making it so that subsequent pulses do not align edge to edge.

5.2.3 IPG Mid Power Scanner (short focal length, 3 mm spot size)

The IPG Mid Power Scanner was tested with two different focal lengths. It was selected due to the possibility of creating a smaller spot size. As originally configured, the smallest spot size achievable was a 3 mm side length square.

This scanner required a third party XY2-100 generator to control the scanner, supplied by UDRI. The device was a Lanmark LEC inside one of Lanmark's Maestro boxes. Titan was unable to configure the standard Bowtie mode using the Linux API to the Maestro box. All IPG scanner tests were performed with the standard zig-zag mode, moving a single mirror back and forth, as opposed to the speed-adjusted mode achievable with the RTC4 card that ensures all lines are parallel.

5.2.4 IPG Mid Power Scanner (long focal length, 1.94 mm spot size)

For the second configuration of the IPG scanner, a replacement f-theta lens was ordered that generated a 1.94 mm square spot. This was the smallest tested during this set of experiments.

5.2.5 Important Laser / Scanner Parameter Definitions

5.2.5.1 Focus

The intelliWELD scanners have built in focus control. While keeping the physical distance from the scanner to surface constant, this control changes the spot size, shape, and energy distribution. For pulsed lasers, uniform energy distribution is important. Therefore, all tests had the focus set such that the surface was at the focal point. Unfortunately, the beam shaping optic required a focus control that was not set so that the focal point was on the surface to get the smallest spot possible. This spot was closer to a 3 mm diameter circle and did not have uniform energy distribution. The

IPG scanner did not have focus control, so it was adjusted to the desired focus by physically moving the scanner.

5.2.5.2 Spot Shape

The fiber optic cable from the laser has a square core, and the desired spot shape was square. When operating at non-nominal focus, the spot becomes much rounder. Similarly, the beam shaping optic made the spot an ellipse; and when adjusted, a circle. Energy distribution in the spot is also important, as that influences irradiance and radiant exposure. These are two key metrics for achieving the ablation threshold. A non-uniform energy distribution would ablate in the center of the spot but not in the edges. Only the perfect square spots on the surface had a uniform energy distribution.

5.2.5.3 Spot Size and Energy Characteristics

Spot size and energy characteristics are listed in **Table 8** and are dictated by the fiber, scanner, and lens combination. Three different spot sizes were achievable with the hardware at hand. Spot size occupies an interesting position in the parameter space. The larger spots potentially allow for a larger area to be processed, per unit time; but also decrease irradiance, potentially dropping the process below the ablation threshold. Spot size is an important parameter because it directly influences irradiance and radiant exposure on the coatings.

Table 8 Laser Spot Characteristics

Scanner	IW30 460mm		IPG with 254mm lens		IPG with 163mm lens	
	Irradiance (MW/cm^2)	Fluence (J/cm^2)	Irradiance (MW/cm^2)	Fluence (J/cm^2)	Irradiance (MW/cm^2)	Fluence (J/cm^2)
T1	24.49	0.74	14.17	0.43	34.39	1.03
T2	27.54	1.10	15.94	0.64	38.68	1.55
T3	24.49	1.47	14.17	0.85	34.39	2.06
T4	14.69	1.47	8.5	0.85	20.63	2.06

5.2.5.4 Irradiance

The power was observed on a surface per unit area. It was found that higher irradiance values resulted in a more defined plasma layer above the point of ablation. This value needed to meet a threshold for ablation to occur. Below the threshold, very little paint was removed. 10 MW/cm^2 was the minimum required irradiance, though higher values tended to produce better results.

5.2.5.5 Radiant Exposure/Fluence (J/cm^2)

Energy was observed on a surface per unit area. This value was more closely tied with bulk removal rate. Higher radiant exposure led to better removal for the given irradiance.

5.2.5.6 Pulse Overlap

This turned out to be an extremely important parameter. While it was anticipated that subsequent pulses would overlap those preceding, temporal overlap (in addition to spatial overlap) was a key to maximizing removal rate. It was surmised that repeated pulses on an array serve to lower the ablation threshold for those pulses.

5.2.5.7 Galvanometer Speed

Galvanometer speed was the speed at which the spot can be moved across the surface. Larger spots require faster speeds to keep overlap percent the same. Faster speeds were also necessary to process large areas.

5.2.5.8 Cooling delay

After a spot is ablated by the desired number of pulses per row and rows per pass, a certain amount of time should pass, known as the cooling delay, prior to the same point being ablated again. This was meant to allow for residual temperatures to subside.

5.2.5.9 Spot overlap (derived)

The parameter corresponds to a percentage overlap from one spot to the next. The spot path was controlled such that the overlap was in a single direction. It is generally preferred to have the inverse of this value be a whole number (any given point gets hit by the same number of pulses).

5.2.5.10 Row overlap (derived)

Similar to spot overlap, the ablation pattern determined rows of ablation spots. These rows overlapped one another. It is generally preferred to have the inverse of this value be a whole number (any given point gets hit by the same number of rows).

5.3 Closed Loop Metallic Optimization

5.3.1 Panels

Table 9 Aluminum Substrates and Initial Surface Treatments

Substrate ID[1]	Material	Thickness (inch)	Initial Surface Treatment
2024_032_BN	2024-T3	0.032	None
2024_032_BA	2024-T3	0.032	Anodize - MIL-A-8625, Type I, Class 1
2024_032_CC	2024-T3 Clad	0.032	CCC - MIL-DTL-5541, Class 1, Type 1A
1. Last field of ID: BN (bare, no treatment), BA (bare, Anodized), CC (clad, chromate conversion)			

Procurement details are listed here:

1. Both bare and clad aluminum sheet was purchased from UDRI_SPECThyssenKrupp Materials NA Inc.
2. The material suppliers then cut the sheet stock into 18” x 24” panels with 18” dimension parallel to the mill roll direction (**Figure 6**).
3. Pre-treatments (Anodize and Chromate Conversion) were performed by Hohman Plating and Manufacturing from Dayton, Ohio (**Table 9**).
    a. Anodize pre-treatment was applied IAW MIL-A-8625, Type I, Class 1.
    b. Chromate Conversion (alodine) pre-treatment was applied IAW MIL-C-5541, Class 1A.

5.3.2 Coatings

Coatings were applied at the University of Dayton Research Institute IAW the manufacturer instructions. These were then shipped to Titan Robotics for de-painting.

5.3.3 De-Paint

De-painting was conducted at Titan Robotics Inc. in Pittsburgh, Pennsylvania.

5.3.3.1 Enclosure

All testing was performed in a custom laser safe enclosure measuring roughly 8x4x4 feet **(Figure 8**). The laser scanners are swappable, and mounted in the center aiming down at a fixture for test panels riding on a linear rail capable of moving at speeds up to 200mm/s.

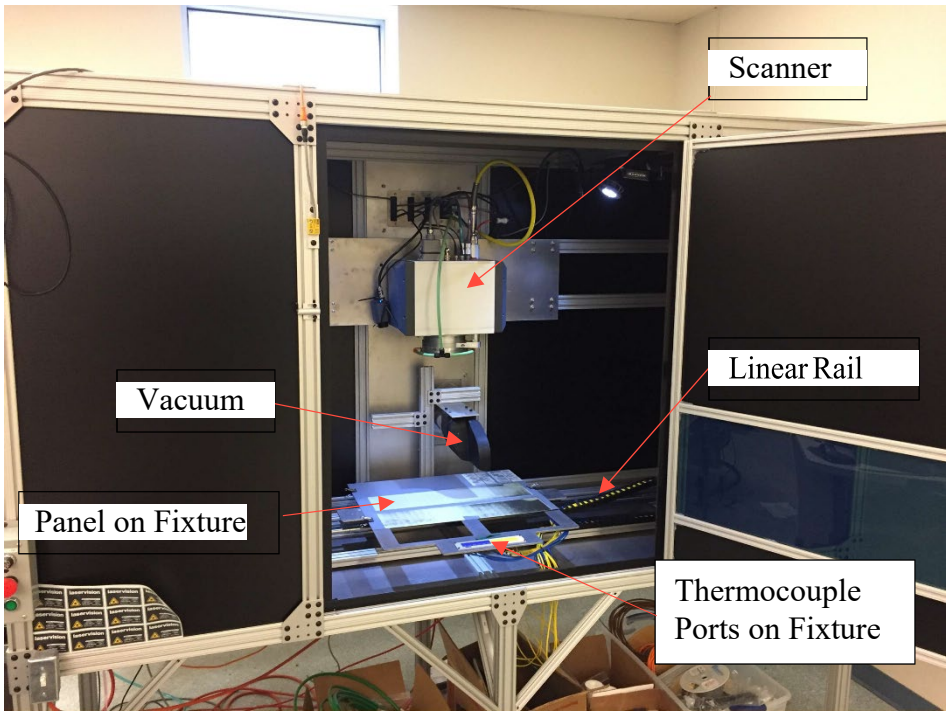

Figure 8 Custom Laser Enclosure

A vacuum nozzle with manual pressure relief valve was installed several inches above the linear rail. The pressure was set to maximum, then adjusted downward until debris / flame from the ablation process was not drawn along the surface and then up into the vacuum. The desired effect had the effluent plume initially starting upward, then directly to the vacuum.

An air knife was employed to keep the cover glass clear. Its pressure was turned up so that it would not allow typical ablation dust / debris from contacting with the cover glass.
Panel speed was controllable via the linear rail up to 200 mm/s. This parameter allowed for the test cell to mimic the speed of a robotic arm over the surface.

5.3.3.2 Laser Parameters

Laser parameters can be set via three mechanisms: laser mode, pulse repetition rate (PRR), and a maximum average power. **Table 10** shows the available laser modes and their associated nominal pulse repetition rate. It is possible to select a maximum power less than 1 kW, though that was not tested as part of these experiments.

Table 10 Laser Pulse Modes

Name	Pulse Duration (ns)	Pulse Energy (mJ)	Nominal PRR (kHz)	Max Pulse Power (MW)
T1	30	50	20	1.667
T2	40	75	13.33	1.875
T3	60	100	10	1.667
T4	100	100	10	1

Pulse Energy: The pulse energy was tied to the currently selected laser mode. If the pulse repetition rate was less than or equal to the nominal rate, the energy per pulse was as stated. If the pulse repetition rate was higher, the energy decreased so that the maximum average power was 1 kW.

Pulse Duration: The pulse duration was tied to the currently selected laser mode. While the laser was actively pulsing, the pulse duration cannot change.

Pulse Repetition Rate: The pulse train the laser generates was configurable from 2 to 50 kHz. The pulses always occurred equally spaced from one another. While the laser was actively pulsing, the repetition rate could change.

Average Power: The maximum average power for the laser used was 1 kW, regardless of pulse mode or pulse repetition rate. This means that for pulse repetition rates higher than the nominal for the mode, the energy per pulse decreased to maintain 1 kW average power. For pulse repetition rates lower than nominal, the average power was lower than 1 kW.

5.3.3.3 Panel Test Plan and Layout

2024 T-3 aluminum panels with the standard Air Force gray topcoat and chromated yellow primer, as well as, the Air Force gloss white topcoat and chromated yellow primer were processed with laser process parameters that satisfied two criteria:

1. Effectively removed topcoat and primer coatings without imparting substrate damage.
2. Pushed up to and beyond the substrate temperature limit of 250ºF imposed by the Air Force.

The panels were initially subdivided into four quadrants, testing each at 60,70,80,90% pulse overlap in the scan direction., The results were compared to the analogous overlaps from the previous testing on global hawk panels. To keep the analogue as close as possible, the pulse repetition rate was held at 10 kHz.

Screening was conducted by subdividing each aluminum test into several separate patches, with each patch subject to a separate set of process parameters. The individual patches would then be further subdivided to approximately 1”x6” (30mmx150mm) regions as shown in **Figure 9**. This would be automatically step masked to provide a variety of exposure levels for each parameter set.

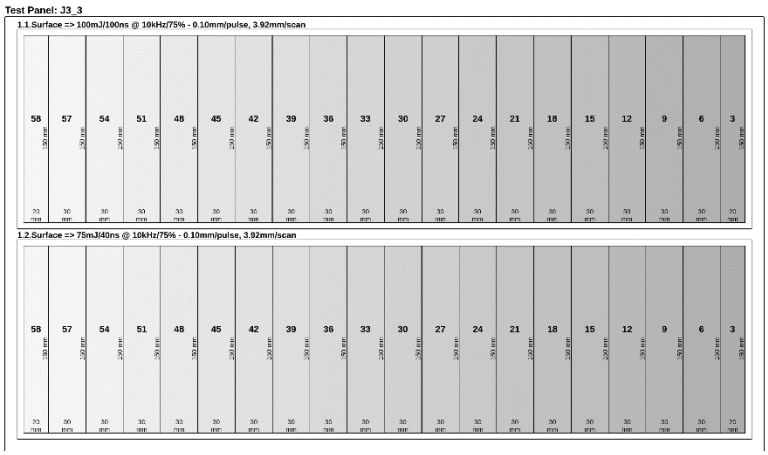

Figure 9 Panel Layout

5.4 Composite Optimization Testing

5.4.1 Materials

A total of three different types of composite panels were created for this testing.

5.4.1.1 Composite Material Selection

Composite materials for optimization and screening were selected from those utilized on the RQ-4 and the C-130 weapon systems. Selected carbon fibers included representatives with high and intermediate strength (modulus). A Kevlar composite provided a low-strength composite representative. Selected resins included both low and high cure-temperature representatives. The service temperature for these materials was 200ºF. The maximum temperature allowable during coating removal was 50ºF below the specified service temperature of the composite resin resulting in the allowed temperature limit of 150ºF (**Table 11**).

Table 11 Composite Material Selection

Panel Type ID	Fiber	Resin	Fiber Type / Modulus (Msi)	Resin Type / Cure Temperature (°F)	Allowed Temp (°F)	Weapon System
M46J	M46J	7714A	Carbon / High (63)	Epoxy / Low (250)	150	RQ-4
T650	T650	F584	Carbon/ Intermediate (37)	Epoxy / High (350)	150	C-130J
285K	285K / 120 Glass	7714	Kevlar (49), Glass / Low (6)	Epoxy / Low (250)	150	C-130J

5.4.1.2 Composite Panel Construction

A thin-skin sandwich construction (honeycomb core between a top skin and bottom skin) was selected to provide high sensitivity to potential degradation of the composite skin by the coating removal process. Prior screening tests utilized thicker laminates, which exhibited lower sensitivity to surface ply degradation because the bulk laminate could carry most of a test load. Potential degradation of the composite matrix was evaluated by measuring long-beam flexure strength. Panel construction (thin-skin honeycomb-core panels, **Figure 10**) followed the guidance of ASTM D7249 and SAE MA4872A (section 5.15). SAE MA4872A specifies a 2-ply/core/3-ply construction to ensure treatment-skin failure during beam flexure testing and provided guidance on honeycomb core selection. ASTM D7249 provided guidance for specification of panel loading span based on the skin and core material properties, providing a bridge between SAE MA4872A (commercial aerospace materials) and the weapon systems materials.

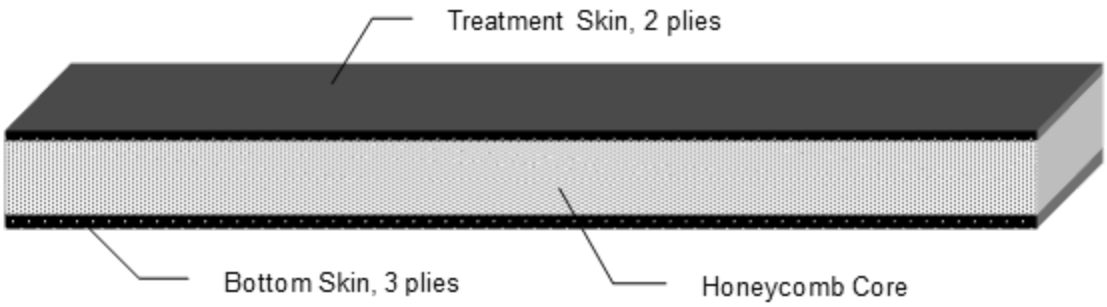

Figure 10 Composite Panel Construction

The top skin on which coating removal will be performed (treatment-skin) consisted of two fabric plies comparable to the thinnest (most sensitive) aircraft OML laminates. The bottom skin had three fabric plies. The sandwich construction was designed to fail within the treatment-side skin. Following ASTM D7249, beam support spans were selected so that during long beam flexure testing, treatment-skin failure occurred before core shear failure with at least a 25% margin. Potential composite degradation by the LCR process resulted in failure strength reduction of LCR treatment specimens relative to the control specimen. Control specimens were from the same batch of materials as the test articles but did not receive coating or undergo the LCR process.

Panel skin material details are provided in **Table 12**. Skins were composed of fabric plies (either woven or unidirectional) and resin. Skin fabrication followed the OEM specifications listed in **Table 12** and the material manufacturer recommendations.

SAE MA4872A specifies 2 ply and 3 ply skins fabricated from woven fabrics, but M46J fiber was not available in this form. Two plies of M46J unidirectional fabric with 0/90 layup was used in place of a woven fabric ply. Two unidirectional plies yield a 0/90 laminate with 0.28 mm thickness (comparable to that of the selected fabrics). The M46J panel top skin therefore had four plies (0/90) and the bottom skin had six plies.

Sandwich panel component specifications are in **Table 13.** Honeycomb core density, cell size, and thickness followed the guidance of MA4872A.

Table 12 Composite Panel Skin Specification

Skin ID	Fiber	Resin	Specification	Skin ply Fabric			Laminate		
				Weight g/m^2	Weave	Thickness mm	Plies	Layup	TC @ Plies[a]
S4-M46J	M46J	7714A	ACS-MRS-5002	145	Uni[b]	0.14	4	$[0/90]_4$	-
S4T-M46J							4	$[0/90]_4$	2-3
S6-M46J							6	$[0/90]_6$	-
S2-T650	T650	F584	STM22-817 Type 1 Class 2	193	Plain	0.18	2	$[0/90]_2$	-
S2T-T650							2	$[0/90]_2$	1-2
S3-T650							3	$[0/90]_3$	-
S2-285K	285K/ 120 glass[c]	7714	STM-22-912	173	4H Satin	0.254	3	$[0/90]_3$	-
S2T-285K				105		0.089		$[0/90]_3$	1-2
S3-285K	258K			173		0.254	3	$[0/90]_3$	-
(a) Thermocouples embedded between the indicated plies. For S2T-285K, between 120 glass and Kevlar plies.									
(b) Unidirectional tape.									
(c) 2 plies of Style 285 Kevlar + 1 ply Style 120 e-glass (tool side)									

Table 13 Composite Panel Sandwich Specification

Panel Type ID	Panel Quantity	Top Skin (tool side)	Bottom Skin	Core				Core / Skin Adhesive
				Part Number[(a)]	Cell Size Inch	Density lbs/ft^3	Thickness Inch	
P-M46J	13	S4-M46J	S6-M46J	HD183	1/8	8	1/2	AF163-2M
PT-M46J	8	S4T-M46J	S6-M46J					
P-T650	6	S2-T650	S3-T650					
PT-T650	2	S2T-T650	S3-T650					
P-285K	6	S2-285K	S3-285K	HD343	3/16	4	1/2	
PT-285K	2	S2T-285K	S3-285K					
(a) Gillcore part numbers								

5.4.1.3 Composite Test Panel Fabrication

Specific details on test panels and specifications related to composite panel fabrication are listed below:

1. Test panel size and construction was specified to support extraction of test specimens needed for screening tests. Process optimization test panels were the same size and construction as screening test panels except for the inclusion of embedded thermocouples for substrate temperature measurement.

2. The treatment-skin face was the tool side when the skin laminate or panel sandwich was cured.

3. Panel fabrication process was:

    a. Skin laminates were fabricated/cured and then adhesively bonded to the panel core.

    b. Scotch-Weld AF 163-2M Film, (red at 9.5 mils), was used to bond the cured skin laminates to the honeycomb core.

    c. The core ribbon direction, shown in **Figure 11**, was marked on the bottom skin of the panel.

4. Nominal test panel size was 24” (L-direction, core ribbon) x 24” (W-direction).

5. Panels were fabricated with 30-gauge thermocouples (Omega Engineering PN 5TC-TT-T-30-72) embedded between the first and second fabric plies of the treatment-face skin. Embedded thermocouples in M46J panels were placed between the second and third tape ply of the four-ply treatment face skin (**Figure 12**). The thermocouples supported substrate temperature measurements during process optimization testing to ensure that acceptable substrate temperatures were not exceeded.

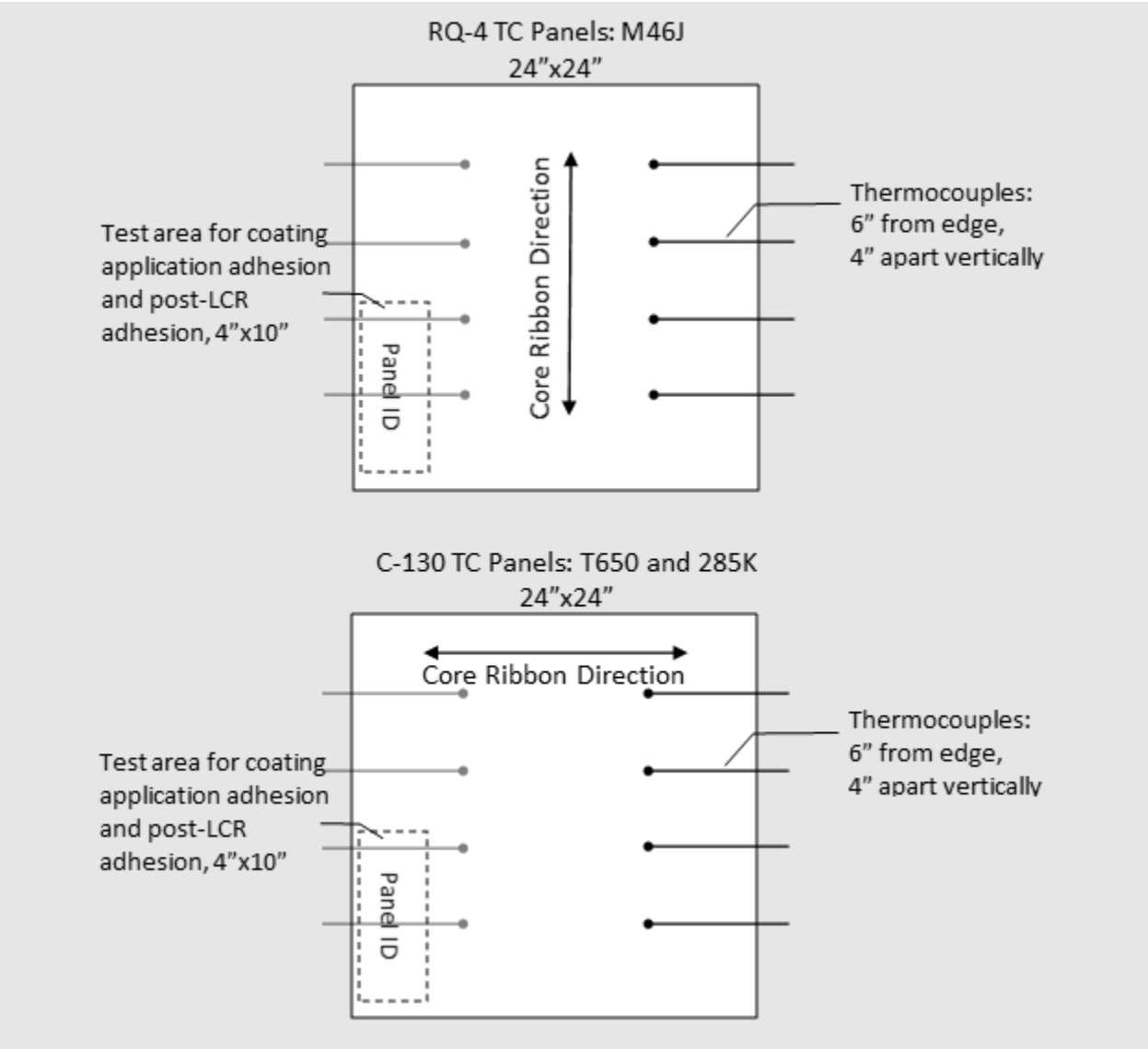

Figure 11 Composite Optimization Test Panel Construction

Panels were sourced / fabricated by the suppliers as indicated in **Table 14 .** The process step of embedding the thermocouples in the top face sheet is shown in **Figure 12**.

Table 14 Panel Material Source Information

Panel Identifier	laminates	Core	Adhesive
M46J	Aviation Equipment Processing	Gill Corporation	Aviation Equipment Processing
T650	Stelia North America	Gill Corporation	Aviation Equipment Processing
285K	Quickstep	Gill Corporation	Aviation Equipment Processing

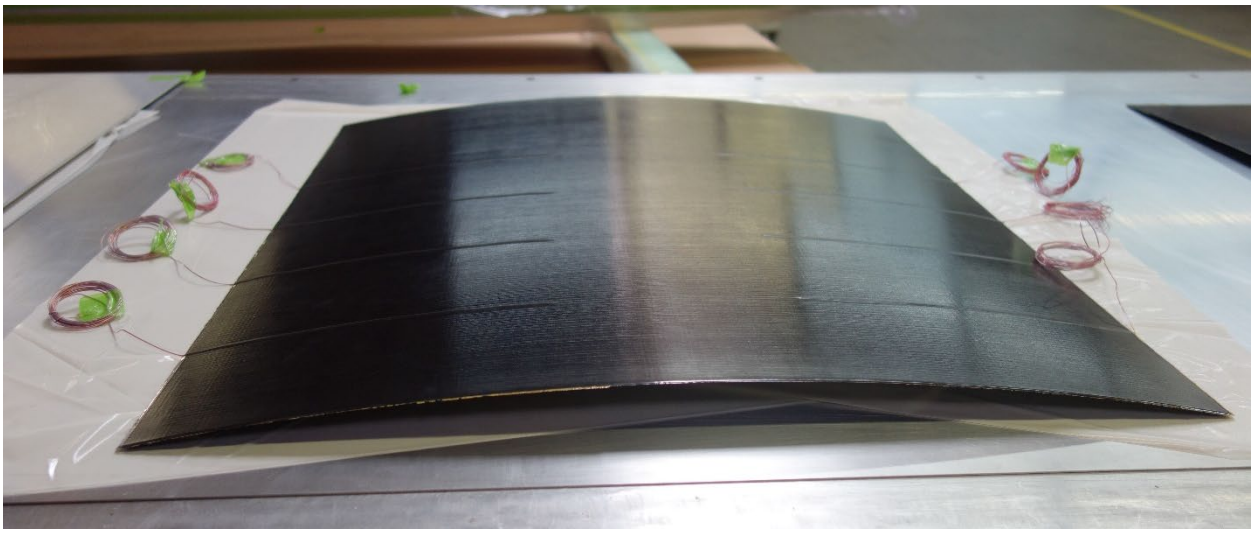

Figure 12 M46J process side laminate skin with thermocouples embedded

5.4.2 Panel Preparation and Coatings

Coating application was performed by Automotive and Industrial Supply in Utah. An overview of composite coating for all 12 optimization panels is shown in **Table 15**. A complete description of materials used, and processes are provided in the following subsections.

Table 15 Panel Preparation and Coating Summary

	Panel ID	Surface Prep	Coating
RQ-4 Representative	M46J_T_0_G_NPF_1,2	Light sand and alcohol wipe	Gray
	M46J_T_S_G_NPF_1,2	Light sand and alcohol wipe, Surface sealer	Gray
	M46J_T_0_GT_NPF_1,2	Light sand and alcohol wipe	Thick Gray
	M46J_T_0_W_NPF_1,2	Light sand and alcohol wipe	White
C-130 J Representative	285K_T_0_G_NPF_1,2	Light sand and alcohol wipe	Gray
	T650_T_0_G_NPF_1,2	Light sand and alcohol wipe	Gray
Panel ID indicates composite material, presence of thermocouples, surfacer, coating stack up, laser process, and panel number. Panel IDs ending with "1,2" indicate that there will be two panels, one receiving panel number 1, and the other receiving panel number 2.			

5.4.2.1 Panel Preparation

The following preparation process was executed prior to the initial coating application on composite panels:

1. Surface was wiped with isopropyl alcohol to remove residual mold release.
2. Manual sanding of the treatment surface (top side) with 220 grit (or finer) abrasive paper to promote primer adhesion was performed.
3. Surface was wiped with wet (isopropyl alcohol) cheesecloth to remove sanding residue.
4. Surface cleanliness was tested to water-break-free condition.

5.4.2.2 Surface Sealer

For the two panels requiring surface sealer, CA 8620 HS PU, Manufacturer, was applied IAW the manufacturer instructions.

5.4.2.3 Primer Application

MIL-PRF-23377 Type I Class C2 primer was used on all panels. Primer application was performed using a High Velocity Low Pressure spray gun IAW TO 1-1-8 and the manufacturer instructions to a dry film thickness of 0.6 – 0.9 mils.

5.4.2.4 Top Coat Application

MIL-PRF-85285, Type IV Class H gray top coat (color 36173) and white top coat (color 27925) were used as listed in **Table 16**. Application was performed using a High Velocity Low Pressure spray gun IAW TO 1-1-8 and the manufacturer instructions.

5.4.2.5 Thick Coatings

For the two panels listed in **Table 15,** as having "thick gray" coatings, this meant a total of 4 stack ups of coating were applied. Surface preparation, primer application, and gray top coat application were performed as previously described. Next, the primer application, top coat application, and accelerated cure steps were repeated 3 more times to reach the total 4 stacks.

5.5 Composite Screening Testing

5.5.1 Materials

Panels were manufactured by the same suppliers and at the same time as the panels previously described with the exception of thermocouples. No thermocouples were used for the screening panels.

5.5.2 Panel Preparation and Coatings

Table 16 Panel Preparation and Coating Information

	Panel ID	Masked area	Surface Prep	Coating
RQ-4 Representative	M46J_0_0_G_NPF_1	Y	Light sand and alcohol wipe	Gray
	M46J_0_S_G_NPF_1	Y	Light sand and alcohol wipe, Surface sealer	Gray
	M46J_0_0_GT_NPF_1	Y	Light sand and alcohol wipe	Thick Gray
	M46J_0_0_W_NPF_1	Y	Light sand and alcohol wipe	White
	M46J_0_0_0_ctl_ctl	Control Panel: No coatings; cure cycles only		
C-130 J Representative	285K_0_0_G_NPF_01	Y	Light sand and alcohol wipe	Gray
	285K_0_0_0_Ctl_Ctl	Control Panel: No coating; cure cycles only		
	T650_0_0_G_NPF_01	Y	Light sand and alcohol wipe	Gray
	T650_0_0_0_Ctl_Ctl	Control Panel: No coating; cure cycles only		
Panel ID indicates composite material, presence of thermocouples, surfacer, coating stack up, laser process, and panel number. IDs showing 1, 2 indicate that there will be two panels, one receiving panel number 1, and the other receiving panel number 2. There is a total of 9 panels represented in this table.				

Coating application was performed in the same manner as previously described, with the exception that a portion of the panel was masked for primer adhesion testing. Masking was performed with 3M painter's tape over the top left corner of the panel as shown in **Figure 13**.

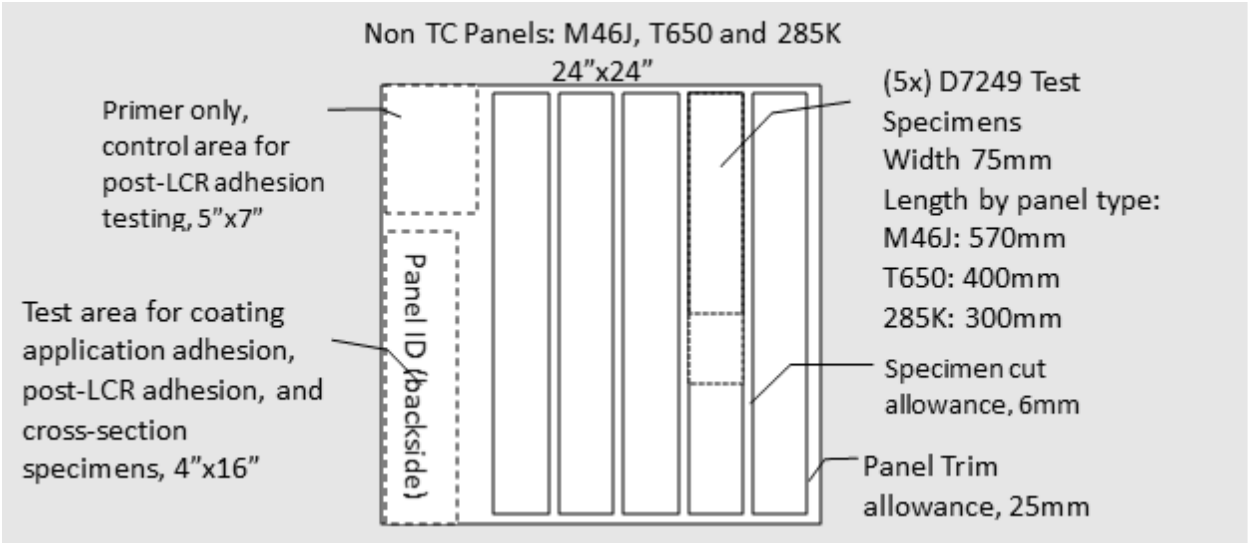

Figure 13 Composite Screening Panel Layout and Cut Plan

In addition, 3 panels remained uncoated, but were subjected to the same cure cycles as the coated panels. These panels were used as control panels during material properties testing.

5.5.3 De-Paint

Panels were completely de-painted at Titan robotics according to the selected optimized parameters.

5.6 Demonstration

A demonstration plan was not generated because the program was brought to a close early by ESTCP.

6.0 PERFORMANCE ASSESSMENT

6.1 Metallic Open Loop Optimization Testing

Preliminary review of results from **Table 5** - Test Matrix 1 (Groups A-D) indicated that the low-fluence configurations (50% spot and scan steps) yielded higher efficiencies and lower temperatures than higher-fluence parameters. The best efficiencies were comparable, thus a 100 mJ pulse energy provided a greater strip rate than the 75 or 50 mJ pulse energies. A 60 ns pulse duration with a 50% spot and scan step was therefore selected as the reference configuration for testing alternate spot sizes. The trend of higher efficiencies from lower fluence levels suggested that spot sizes larger than 1.6 mm be tested. A test matrix (**Table 6**, 2.0 and 2.3 mm spot sizes) was configured to obtain a pass fluence comparable to the reference configuration (1.6 mm spot size) by increasing spot size and decreasing spot or scan step. Since spot and scan steps are constrained (to 1/N), the 2.0 and 2.3 mm spot sizes were calculated as those which provided scan fluence equivalent to the reference configuration for spot steps of 1/3 and 1/4, respectively. Given a scan fluence comparable to the reference configuration, a scan step equal to the reference (50%) yields an equivalent pass fluence. In addition, use of a 50% spot step for the 2.0 and 2.3 mm spot sizes allow scan steps of 1/3 and 1/4, respectively, to be utilized to obtain the same pass fluence. This conveniently enabled a trade-off comparison between greater spot step or scan step at the same fluence.

Table 17 Trade-Off Comparison

Pulse Duration	Spot Size	Spot Step	Scan Step	Time between passes
	1.6mm	50% overlap	50% overlap	1 min

6.2 Scanner Selection Testing

The SCANLAB IntelliWELD 30 scanner was chosen because the project team was familiar with the scanner control protocols and operational characteristics, many of which were specifically beneficial to various aerospace coating removal operations. The intelliWELD 30 scanner includes an articulated collimator that enabled automated control of the focal properties of the beam enabling optimization of coatings removal at maximum substrate temperatures with acceptable surface finish. It also supported real-world applications by enabling just-in-time correction of the focal field to account for curved surfaces. This was due to the scanner's articulated optical Z-Axis, which allowed for automated focus exploration. This yielded a critical understanding of the sensitivity of pulsed laser use on a full aircraft. Given that the Titan team was extremely familiar with this scanner, this reduced integration risk for the program (**Table 18).**

Table 88 Area Coverage Rates by Scanner

	Max Coverage Rate (ft^2/min)		
Row Overlap (%)	IW30 460mm FL	IPG 254mm FL	IPG 163mm FL
0	14.47314	4.892193	1.566147
50	7.23657	2.446096	0.783074
66.67	4.82438	1.630731	0.522049
75	3.618285	1.223048	0.391537

6.3 Metallic Closed Loop Optimization Testing

6.3.1 Gray Topcoat

Most tests were performed on standard 0.032" aluminum gray panels. However, several different substrate treatments (clad, anodized, bare); and thicknesses (0.040", 0.032", 0.016") were used. These differences did not affect the removal rates. However, 0.016" panels read higher backside temperatures.

6.3.2 White Topcoat

A limited number of tests were conducted on gloss white panels as well. These white panels exhibited very similar removal rates as the gray panels. However, the white panels required a higher irradiance threshold to be met to effectively remove coating.

6.3.3 Multi-Layer Gloss-White/Yellow Stackup

Initial work was performed on multi-layer gloss-white/yellow stackups on 2024 aluminum. The effective coating removal was achieved on these panels using process parameters more aggressive than on gray topcoat using the current experimental setup. However, temperatures were elevated, and the net result showed a great deal of soot/charring, suggesting that we may be approaching the optical limit of this experimental setup. Further investigation of this issue was under way with the current scanner, and discussions were being opened with SCANLAB about alternate optical configurations of this otherwise very capable scanner. Alternate scanners were also being evaluated, including a scanner from IPG that was originally paired with the laser generator for early testing. While not appropriate for large-scale field use, it did have optics that produced a smaller spot size and theoretically better coating removal results.

Some of the time allotted for screening and optimization was spent learning about each of the parameters and how they interact with one another. **Table 19** shows recipes or system parameters tested with the IntelliWELD scanner with no beam shaping optic. These tests were performed on 0.032" bare aluminum panels measuring approximately 18x24 inches. These panels had initial coating thicknesses of 3-5 mils.

For these tests, 300°F was the maximum acceptable temperature. This number was selected based on temperature limit discussion from the systems deployed at Hill Air Force Base. Several recipes were under this threshold.

The desired removal rate was 10 ft^2*mils /min, which is the topcoat removal rate of the system deployed at Hill Air Force Base. All recipes fell short of this mark by a substantial amount. The fastest removal rate observed was 0.79 ft^2*mils/min, of the recipes that were under temperature. This was more than 10x slower than the 6 kW continuous wave system.

Table 19 Selected IntelliWELD30 Recipes (All panels 0.032" Bare Aluminum)

Recipe	Coating	Pulse Duration	Pulse Energy	Pulse Repetition Rate	Galvo Speed	Panel Speed	Ablated Width	Coverage Rate	Max Temp	Removal Rate	Removal Rate	Almen Strip Reading
		S	mJ	kHz	mps	mps	cm	ft^2/min	°F	Mils/pass	ft^2*mils/min	Δmm
T1	Gray	30	50	20	1	0.007	14	0.63	230	0.64	0.4	-0.009
T2	Gray	40	75	13.33	1	0.007	14	0.63	275	0.88	0.55	-0.014
T3	Gray	60	100	10	1	0.007	14	0.63	290	1.25	0.79	-0.017
T4	Gray	100	100	10	1	0.007	14	0.63		1.125	0.71	-0.019
T3-20kHz	Gray	60	50	20	1	0.007	14	0.63	421	1.6	1.01	-0.014
T3-20kHz-gap	Gray	60	50	20	2	0.007	14	0.63	263	0.6	0.38	-0.012
T3-2x	Gray	60	50	20	2	0.014	14	1.26	284	0.58	0.73	-0.01
T1	White	30	50	20	1	0.007	14	0.63	252	0.19	0.12	-0.007
T2	White	40	75	13.33	1	0.007	14	0.63	308	0.34	0.21	-0.012
T3	White	60	100	10	1	0.007	14	0.63	308	0.5	0.32	-0.016
T4	White	100	100	10	1	0.007	14	0.63	307	0.24	0.15	-0.019

6.4 Composite Optimization Testing

Coating removal settings were evaluated by three main criteria described in the following subsections.

6.4.1 Coating Removal Rate (ft^2-mils/min)

One of the fundamental metrics for success was the Volumetric Removal Rate which was typically measured as:

$$Removal\ Rate = \frac{Ablation\ Width * Panel\ Speed}{Mils\ Removed}$$

To perform this calculation, coating thickness was measured using a DeFelsko PosiTector 6000 magnetic and eddy current sensor. The measurement was taken before and after removal, as well as at all steps on the step mask.

6.4.2 Maximum Temperature

As with the continuous wave process, there existed an upper acceptable threshold for substrate temperature. This temperature was measured via thermocouples affixed to the backside of the substrate.

6.4.3 Visual Inspection

A visual inspection was performed to quickly ensure settings did not obviously damage substrates.

These tests were performed to select appropriate laser parameters for coating removal without imparting damage to the substrate as described in section 5.0. Final selected parameters are shown in **Table 20**.

Table 20 Selected Laser Coating Removal Parameters for Composite Substrates

Pulse Duration (ns)	Pulse Energy (mJ)	Pulse Rate (kHz)	Scan Speed (m/s)	Panel Speed (m/s)	Line Spacing (mm)
60	100	2.5	1.5	0.006	1.25

The following Tables (21-26) and Figures (14-20) show the different parameter sets that were used on the composite panels:

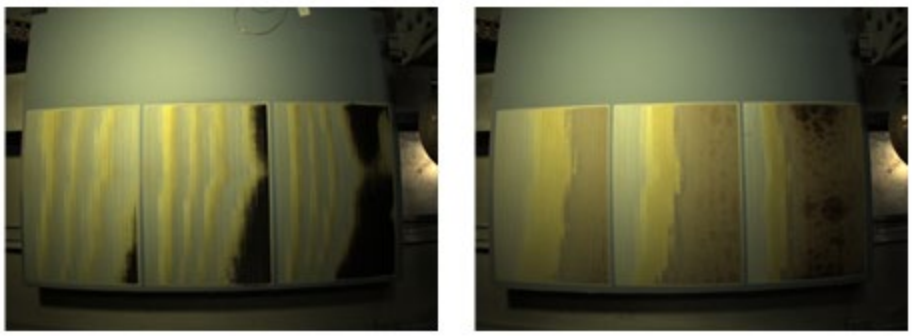

Figure 14 Initial testing panels with embedded thermocouples

Table 21 285 K Single Gray Coating Results

	Pulse Duration (ns)	Pulse Energy (mJ)	Pulse Rate (kHz)	Scan Speed (m/s)	Panel Speed (m/s)	Line Spacing (mm)	Number Passes	Max Temp (°F)
A	60	100	5	1	0.003	2	19	188
B	60	100	5	0.5	0.003	2	16	263
C	60	100	2.5	0.5	0.003	2	19	
D	60	100	5	2	0.002	2	19	
E	60	100	5	2	0.002	1	19	145
F	60	100	5	2	0.002	1.5	19	134
G	60	100	10	3	0.01	1.5	9	
H	60	100	10	3	0.01	1.25	9	207
I	60	100	10	3	0.009	0.3	10	

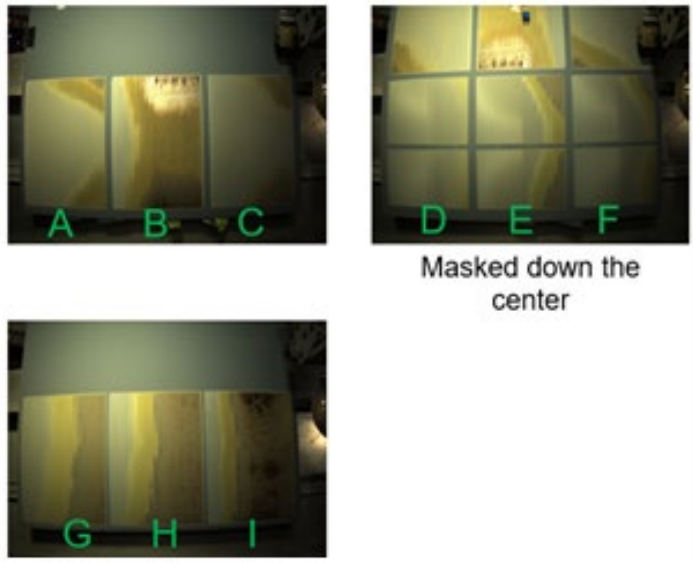

Figure 15 285 K Single Gray Stackup

Table 22 M46J Single Gray Coating Results

	Pulse Duration (ns)	Pulse Energy (mJ)	Pulse Rate (kHz)	Scan Speed (m/s)	Panel Speed (m/s)	Line Spacing (mm)	Number Passes	Max Temp (°F)
A	60	100	10	4	0.012	1	10	254
B	60	100	20	4	0.012	1	19	230
C	60	100	5	2	0.006	1	10	Not Recorded
D	60	100	20	4	0.012	1	15	Not Recorded
E	60	100	2.5	1	0.003	1	5	244
F	30	50	20	4	0.012	1	15	231
G	100	100	10	1	0.003	1	3	468
H	60	100	10	1	0.003	1	3	472
I	40	75	13.33	1	0.003	1	3	515
J	30	50	20	1	0.003	1	3	538
K	100	100	10	0.8	0.003	1	4	400
L	100	100	10	0.9	0.003	1	2	593
M	30	60	40	2	0.003	1	6	307
N	30	60	30	1.5	0.003	1	3	354

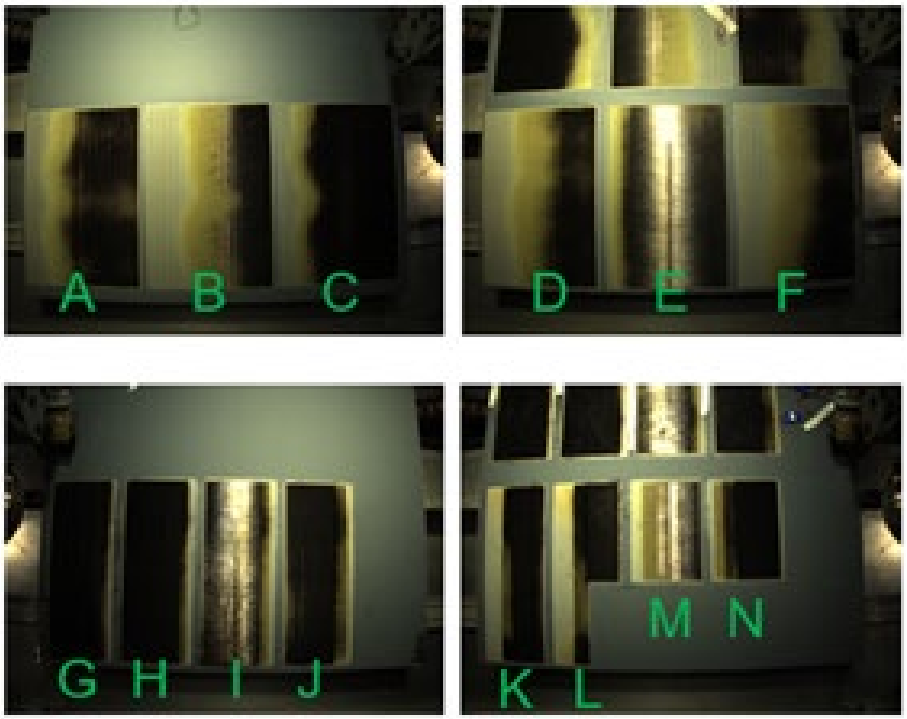

Figure 16 M46J Single Gray Stackup

Table 23 M46J Quad Gray Coating Results

	Pulse Duration (ns)	Pulse Energy (mJ)	Pulse Rate (kHz)	Scan Speed (m/s)	Panel Speed (m/s)	Line Spacing (mm)	Number Passes	Max Temp (°F)
A	60	100	10	3	0.003	1.5	18	107
B	60	100	7.5	2.25	0.003	1.5	18	165
C	60	100	5	1.5	0.003	1.5	18	Not Recorded
D	40	75	13.33	1	0.004	2	20	473
E	40	75	6.66	1	0.004	2	20	229
F	60	100	5	5	0.04	0.4	20	Not Recorded
G	60	100	10	3	0.01	1.5	48	Not Recorded
H	60	100	10	3	0.01	1.25	48	173
I	60	100	10	3	0.01	1	48	210

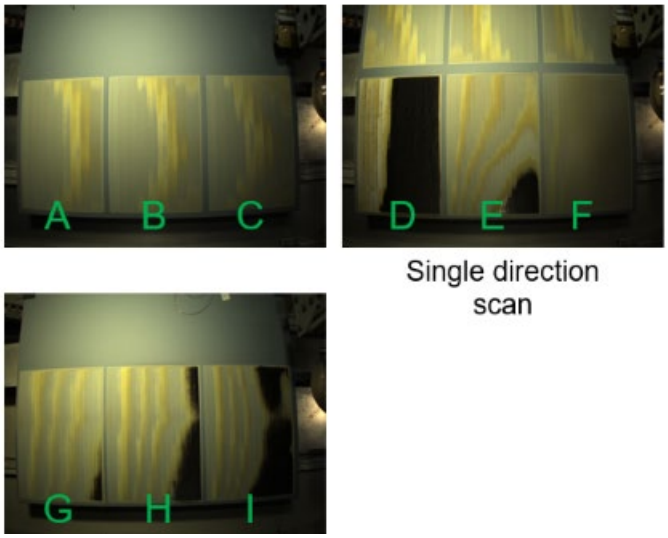

Figure 17 M46J Quad Gray Stackup

Table 24 M46J White Coating Results

	Pulse Duration (ns)	Pulse Energy (mJ)	Pulse Rate (kHz)	Scan Speed (m/s)	Panel Speed (m/s)	Line Spacing (mm)	Number Passes	Max Temp (°F)
A	60	100	10	1.5	0.0045	1	8	Not Recorded
B	60	100	10	2	0.006	1	8	Not Recorded
C	30	50	20	2	0.006	1	9	143
D	30	60	7.5	1.5	0.0045	1	10	268
E	30	60	15	1.5	0.0045	1	10	277
F	30	60	20	1.5	0.0045	1	10	Not Recorded
G	30	60	10	5	0.015	1.25	19	130
H	30	60	10	3	0.009	1.25	19	120
I	30	60	10	4	0.012	1.25	19	Not Recorded
J	30	60	5	2	0.006	1	19	Not Recorded
K	30	60	10	2	0.006	1	8	351
L	30	60	2.5	1	0.006	1	19	199

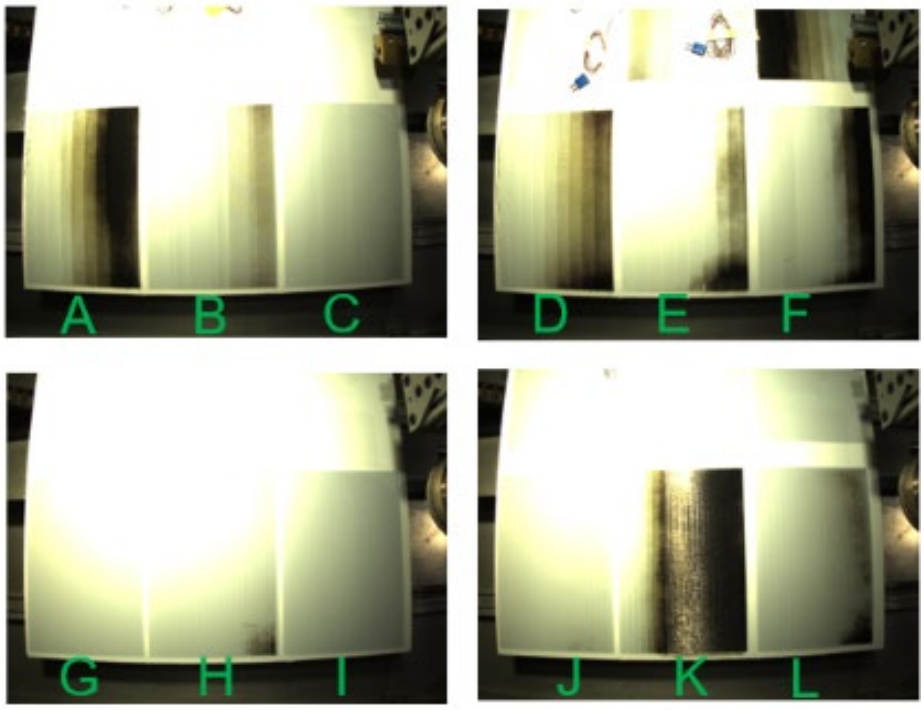

Figure 18 M46J White Stackup

Table 25 M46J Singe Gray with Surface Sealer Results

	Pulse Duration (ns)	Pulse Energy (mJ)	Pulse Rate (kHz)	Scan Speed (m/s)	Panel Speed (m/s)	Line Spacing (mm)	Number Passes	Max Temp (°F)
A	100	100	10	1	0.003	1	9	447
B	60	100	10	1	0.003	1	8	338
C	40	75	13.33	1	0.003	1	8	344
D	30	60	20	1	0.003	1	7	372
E	60	100	2.5	1.5	0.006	1.25	19	143
F	60	100	10	3	0.01	1.25	19	183

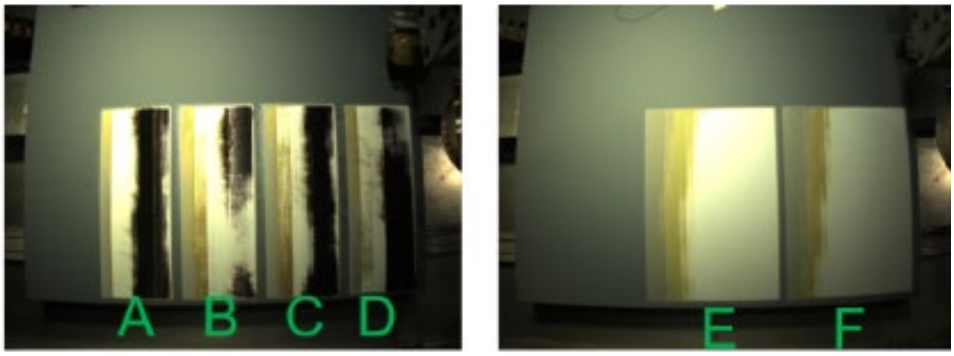

Figure 19 M46J Single Gray with Surface Sealer Results

Table 26 T650 Single Gray Results

	Pulse Duration (ns)	Pulse Energy (mJ)	Pulse Rate (kHz)	Scan Speed (m/s)	Panel Speed (m/s)	Line Spacing (mm)	Number Passes	Max Temp (°F)
A	100	100	5	1.5	0.006	2	18	184
B	60	100	5	1.5	0.006	2	18	183
C	60	100	5	2	0.002	0.5	9	Not Recorded
D	60	100	2.5	1	0.002	1	13	Not Recorded
E	60	100	10	3	0.003	1.25	13	211
F	60	100	10	2	0.003	1.25	13	250
G	60	100	7.5	1	0.003	1.5	6	330
H	60	100	5	1	0.003	1.5	6	Not Recorded
I	60	100	2.5	1	0.003	1.5	9	Not Recorded
J	60	100	5	2	0.006	1.5	9	Not Recorded
K	60	100	2.5	1	0.003	1.5	6	284
L	60	100	10	4	0.012	1.5	10	174

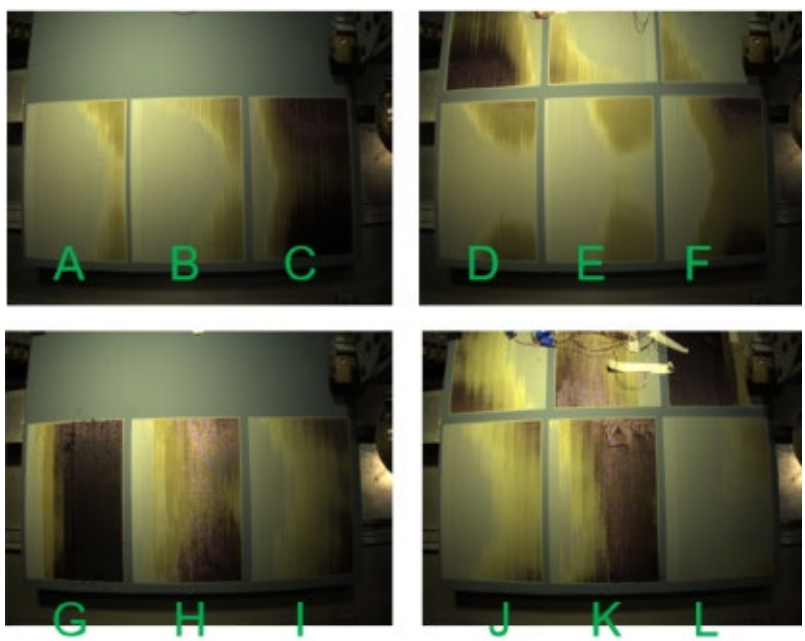

Figure 20 T650 Single Gray Stackup

Ablated panels were then shipped to UDRI for long beam flexure testing.

6.5 Composite Screening Testing

Material property tests were performed on lased and controlled test panels as described in section 5.0. The power settings in **Table 10** were used for all coating removal during this testing. A summary of results is shown in **Table 27,** with photographs of the end state shown in **Figure 21**. Nominal strip rate for these panels was calculated to be 0.97 ft^2mil/min. The nominal strip rate on

the composite panels while meeting the temperature limit of 145°F was approximately 0.97 ft^2mil/min.

Table 27 Composite Screening Material Property Test Results Summary

Panel ID	Num passes	Surface Roughness (Average)	Patti Adhesion (average pull off psig)	Crosshatch Tape Adhesion (Pass: Fail)	Cross Section	Long Beam Flexure (stat. Diff. From control)
M46J_0_0_G_NPF_01	13	2.852	19.2	3:5	Minor surface damage	bottom facesheet effective chord modulus only
M46J_0_S_G_NPF_01	15	3.196	34.1	8:0	No damage	No statistical difference
M46J_0_0_GT_NPF_01	>40	5.597	20.7	7:1	damage	Flexural stiffness only
M46J_0_0_W_NPF_01	not processed; optimized parameters not found by project halt					
M46J_0_0_0_CTL_CTL	N/A	1.834	19.0	0:8	-	-
285K_0_0_G_NPF_01	7	2.368	22.6	8:0	damage	Multiple
285K_0_0_0_CTL_CTL	N/A	1.901	10.6	2:6	-	-
T650_0_0_G_NPF_01	12	2.922	16.3	8:0	damage	Bottom face sheet ultimate stress only
T650_0_0_0_CTL_CTL	N/A	0.829	15.8	3:5	-	-

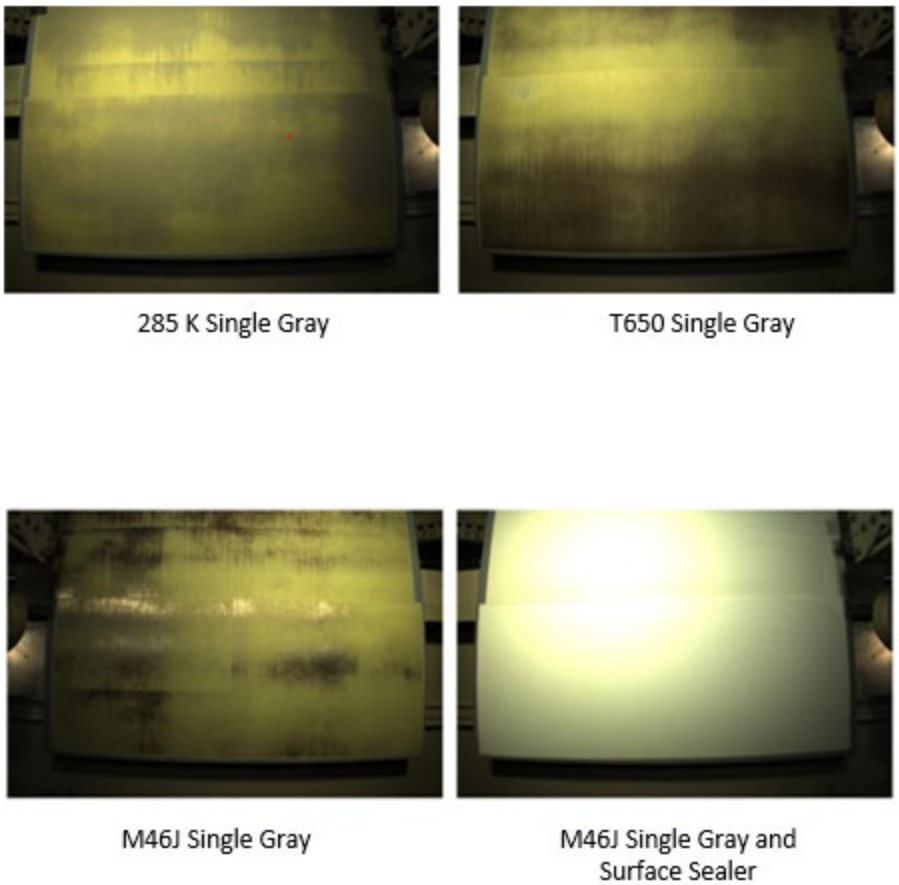

Figure 21 Screening Test Results Visual Post De-paint

6.5.1 Surface Roughness

Surface roughness was conducted using a Mitutoyo SJ-210 Stylus[1] in three separate regions of the test area. Regions were selected to provide data for the range of remaining coating amounts: least amount, a mode amount, and a maximum amount. Five measurements were taken in each location: 3 perpendicular to the core direction, and 2 parallel. Measurement set up is shown in **Figure 22.**

Additionally, a magnified image was taken of each measurement region using a Keyence VR-3200 Height scale, which was 3.5 magnification. Keyence set up as well as sample data is provided in **Figure 23**.

[1] Serial number 502831709, last calibration date of 3/27/2019 valid for one year. Measurement date 18 Dec 2019

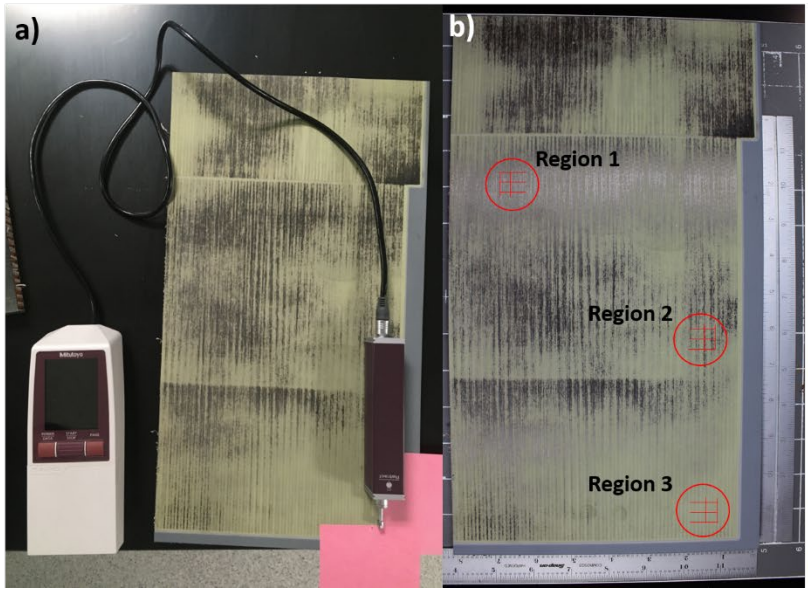

c)

M46J_0_0_G_NPF_01					
Region 1 - Least Coating Removal					
	Ra	Rz	Rp	Rv	Rt
LCR Perpendicular 1	2.048	14.037	7.069	6.969	17.376
LCR Perpendicular 2	2.549	15.917	8.206	7.711	24.709
LCR Perpendicular 3	1.928	14.815	8.265	6.551	24.845
LCR Paralle 1	2.497	16.983	9.450	7.533	28.886
LCR Paralle 2	2.858	20.092	8.290	11.802	23.279
Avg. Perpendicular	**2.175**	**14.923**	**7.847**	**7.077**	**22.310**
Avg. Parallel	**2.678**	**18.538**	**8.870**	**9.668**	**26.083**
Avg. Overall	**2.376**	**16.369**	**8.256**	**8.113**	**23.819**

Region 2 - Mid Coating Removal					
	Ra	Rz	Rp	Rv	Rt
LCR Perpendicular 1	2.063	13.132	7.062	6.070	15.382
LCR Perpendicular 2	3.662	22.166	11.781	10.385	31.479
LCR Perpendicular 3	2.507	15.677	8.285	7.392	28.351
LCR Paralle 1	3.087	19.895	9.105	10.790	22.871
LCR Paralle 2	3.150	18.347	7.296	11.051	20.920
Avg. Perpendicular	**2.744**	**16.992**	**9.043**	**7.949**	**25.071**
Avg. Parallel	**3.119**	**19.121**	**8.201**	**10.921**	**21.896**
Avg. Overall	**2.894**	**17.843**	**8.706**	**9.138**	**23.801**

Region 3 - Most Coating Removal					
	Ra	Rz	Rp	Rv	Rt
LCR Perpendicular 1	2.441	15.517	7.503	8.014	26.308
LCR Perpendicular 2	3.643	23.063	12.612	10.451	30.317
LCR Perpendicular 3	2.467	15.136	8.452	6.684	19.447
LCR Paralle 1	3.175	22.683	10.627	12.056	30.181
LCR Paralle 2	4.703	26.142	12.885	13.258	33.197
Avg. Perpendicular	**2.850**	**17.905**	**9.522**	**8.383**	**25.357**
Avg. Parallel	**3.939**	**24.413**	**11.756**	**12.657**	**31.689**
Avg. Overall	**3.286**	**20.508**	**10.416**	**10.093**	**27.890**

Figure 22 Surface Roughness Testing

a) Mitutoyo Set Up, b) Test Region Locations c) Sample Data

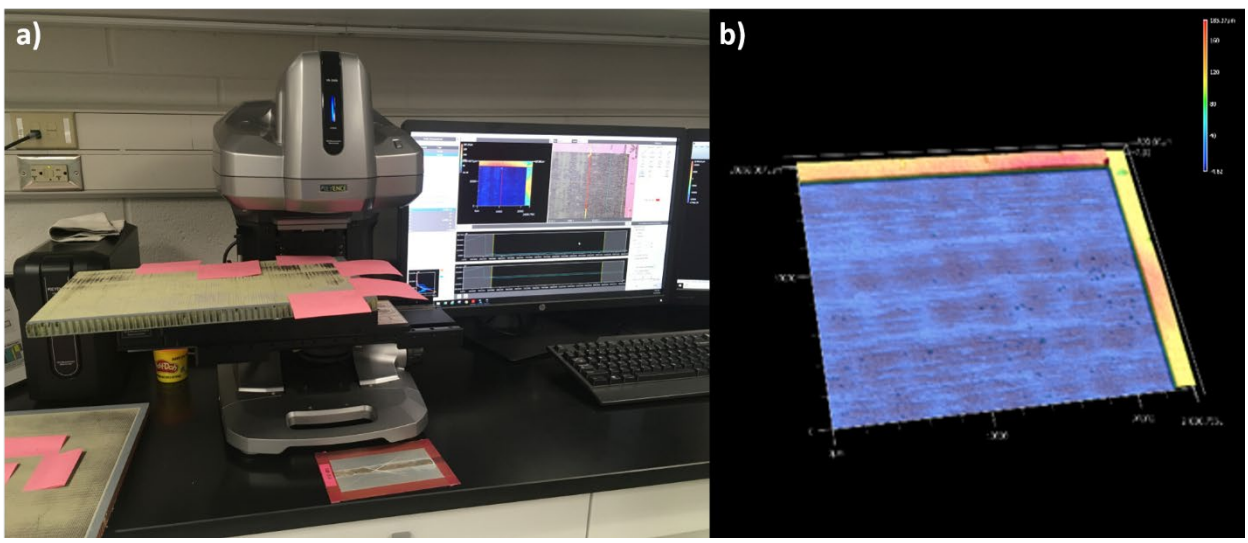

Figure 23 Surface Roughness Imaging

a) Keyence Set Up, b) Sample Image

6.5.2 Primer Adhesion

This test was performed to ensure laser coating removal did not negatively affect an aircraft's capability to be re-coated. De-painted panels were recoated with primer. Next, the primer adhesion was conducted by two methods: ASTM D3359 Method B Crosshatch Tape Adhesion; and ASTM D4541 Patti Adhesion.

6.5.2.1 Crosshatch Tape Adhesion Testing

Adhesion testing was performed by scratching the coating using a 2.0 mm blade and adhering tape to the scribe. Upon removal of the tape, the resulting pattern was visually evaluated for removal of primer in comparison to the classification system from ASTM D3359 (**Figure 24)**. The test results are shown in **Table 28**.

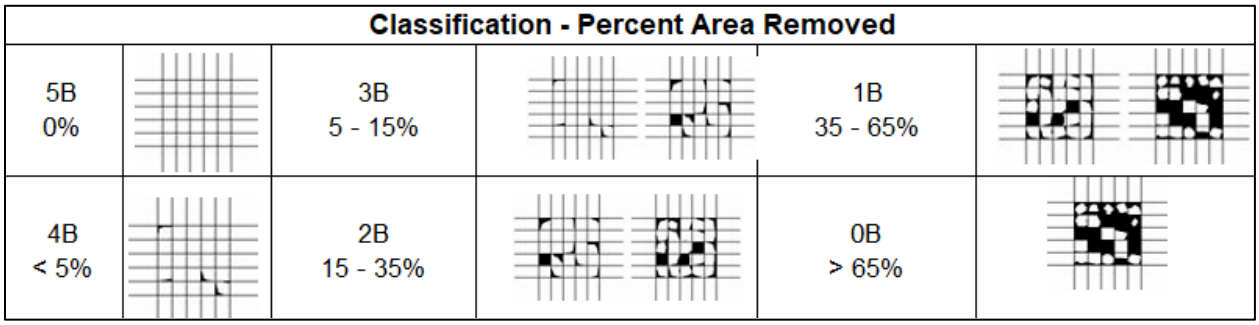

Figure 24 Crosshatch Adhesion Testing Classification System

Table 28 Crosshatch Tape Adhesion Test Results

Panel ID	Classification Results								P:F
	1	2	3	4	5	6	7	8	
M46J_0_0_G_NPF_01	3B	4B	3B	4B	3B	4B	3B	3B	3:5
M46J_0_S_G_NPF_01	5B	5B	5B	5B	5B	5B	5B	5B	8:0
M46J_0_0_GT_NPF_01	4B	4B	4B	4B	3B	4B	4B	4B	7:1
M46J_0_0_W_NPF_01	not processed; optimized parameters not found by project halt								
M46J_0_0_0_CTL_CTL	2B	3B	1B	1B	1B	3B	2B	1B	0:8
285K_0_0_G_NPF_01	5B	5B	5B	5B	5B	5B	5B	5B	8:0
285K_0_0_0_CTL_CTL	2B	4B	3B	3B	2B	2B	2B	4B	2:6
T650_0_0_G_NPF_01	5B	5B	5B	5B	5B	5B	5B	5B	8:0
T650_0_0_0_CTL_CTL	4B	3B	3B	3B	2B	4B	4B	3B	3:5

Interestingly enough, the control samples appeared to have tape adhesion results from the lased samples.

6.5.2.2 Patti Adhesion Testing

Patti Adhesion testing was conducted by adhering a pull stud to the test article and using a pneumatic piston to increase pressure until a failure occurred (with pressure of failure being recorded). The pull stub was visually evaluated to determine the interface that the adhesion failure occurred (**Figure 25**) (**Table 29**).

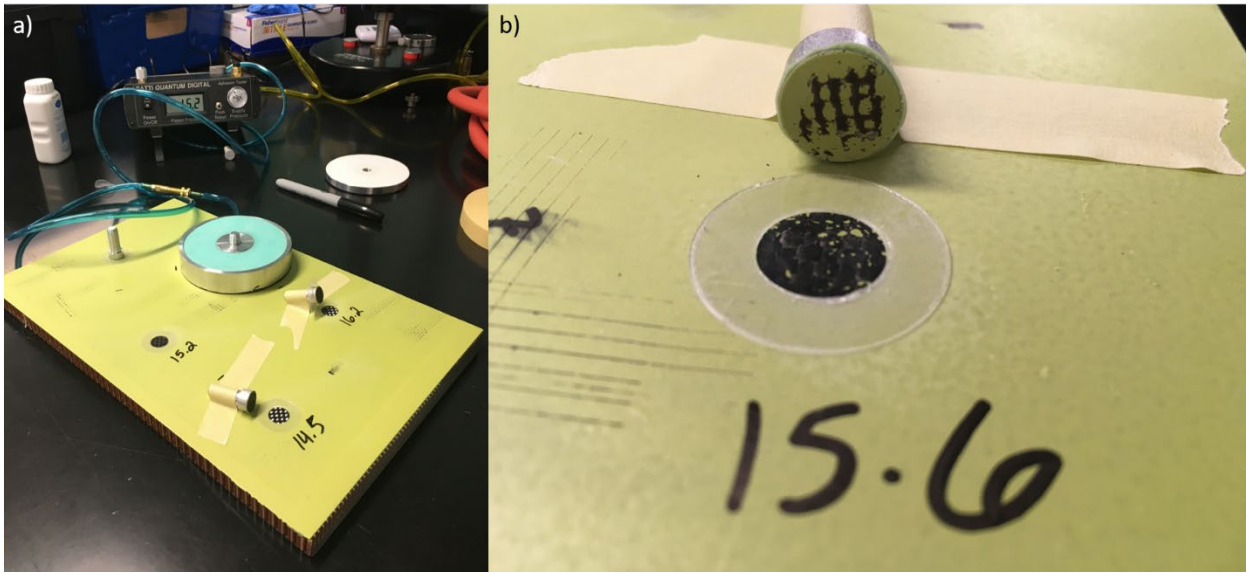

Figure 25 Patti Adhesion Testing

Table 29 Patti Adhesion Test Results

Panel ID	Average Pull off pressure (psig)	Average POTS (Calculated)	Failure mode (most occurring)
M46J_0_0_G_NPF_01	19.2	775.0	Primer to substrate adhesion
M46J_0_S_G_NPF_01	34.1	1378.8	Primer to substrate adhesion
M46J_0_0_GT_NPF_01	20.7	836.4	Primer to substrate adhesion
M46J_0_0_W_NPF_01	not processed; optimized parameters not found by project halt		
M46J_0_0_0_CTL_CTL	19.0	767.5	Primer to substrate adhesion
285K_0_0_G_NPF_01	22.6	915.0	Primer to substrate adhesion
285K_0_0_0_CTL_CTL	10.6	426.8	Primer to substrate adhesion
T650_0_0_G_NPF_01	16.3	658.0	Primer to substrate adhesion
T650_0_0_0_CTL_CTL	15.8	637.7	Primer to substrate adhesion

6.5.3 Cross-Section Visual Inspection

The UDRI metallography lab performed the cross-section visual inspections of all eight composite panels. Among the panels were three control specimens to be compared against the various laser de-painted specimens. The panels were photographed in the as-received condition after being marked to show where samples would be sectioned out for testing. Three samples were taken from each panel. If the panel exhibited variation in the surface condition, the samples were taken from the various regions (e.g. one sample would be taken from a region with paint left over; another from a region with no paint left; and the third from some intermediate spot). The samples were

potted, polished, and examined on a microscope. The locations of each cross section can be seen in **Figure 26** and **Figure 27**.

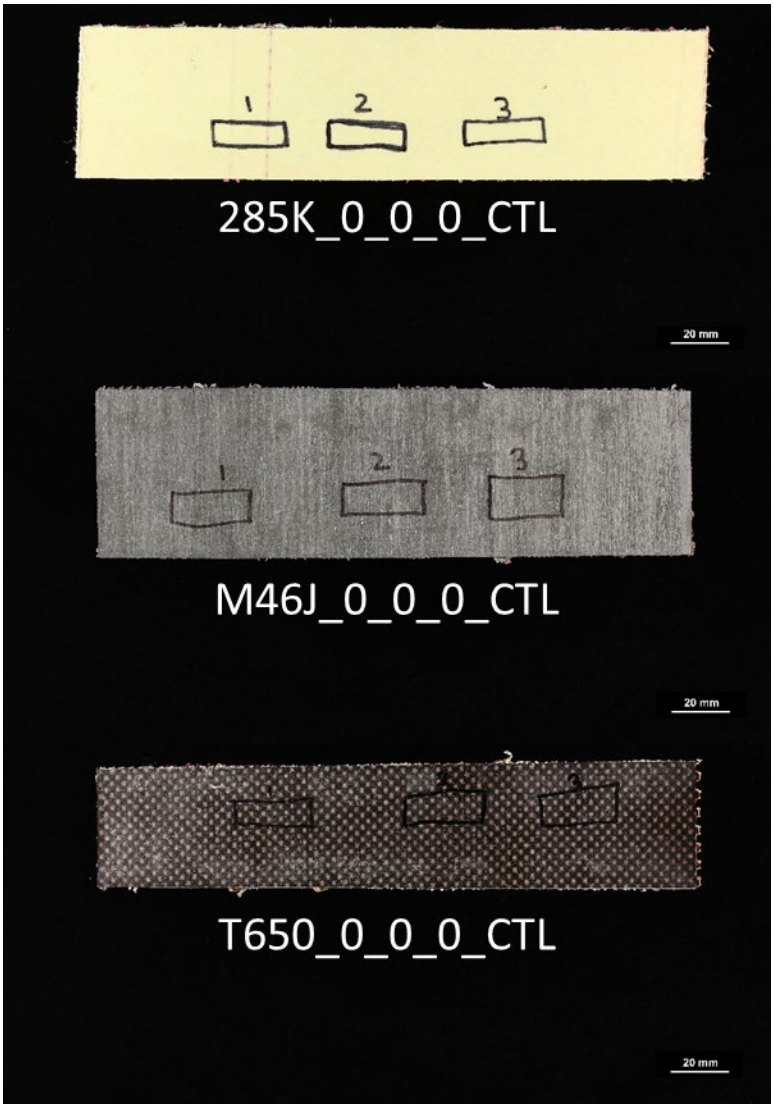

Figure 26 Cross Section Locations of Control Panels

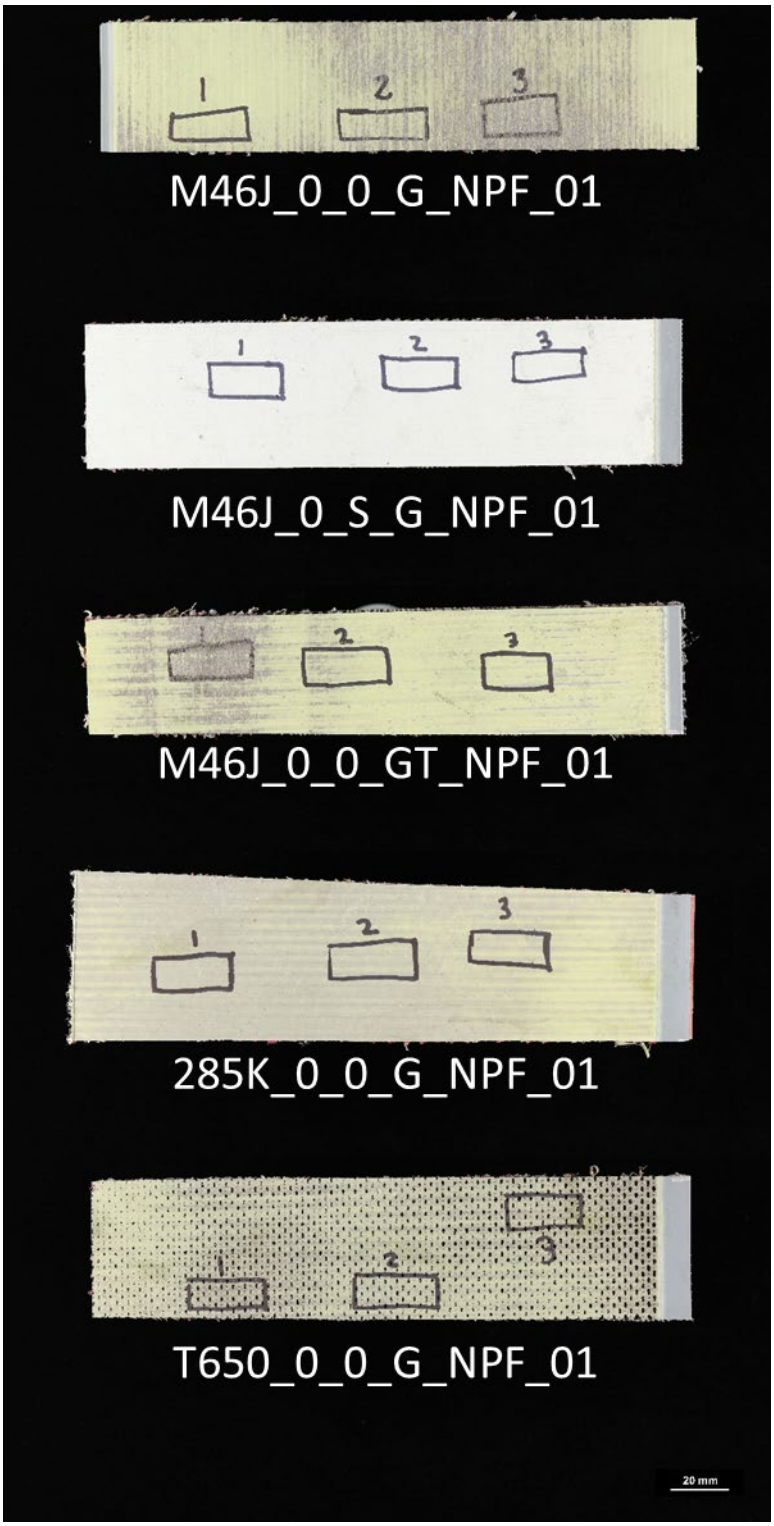

Figure 27 Cross Section Locations of Test Panels

6.5.3.1 Sectioning & Mounting

The panels were sectioned using a diamond blade band saw, with water as a coolant and flushing agent. The first cut was through the thick axis of the panel to separate the front from the back, sectioning through the honeycomb intermediate layer. Samples that were sectioned out around the regions are marked in the macro photographs. Sectioned samples were rinsed with tap water, then rinsed with isopropyl alcohol and blown dry with compressed air. They were then placed into molds and set in a vacuum chamber for at least 10 minutes to further dry out any remaining solvent used to clean them. Struers Epofix epoxy, a two-part slow cure resin and hardener, was used to mount the samples. These were poured in a vacuum to help keep any air from getting trapped within the specimens.

6.5.3.2 Polishing

Polishing was performed using a Struers Tegramin-30, automated polisher. When control specimens existed, they were placed into the same polishing jig as their test counterparts. This ensured both conditions received the exact same polish. Plane grinding was accomplished using silicon carbide papers with water as a coolant. Fine grinding was carried out using 1200 grit silicon carbide. Polishing was done in three steps using Struers Red lubricant (an oil in water emulsion) as follows:

1. 3µm diamond on low nap woven acetate (Struers Dac)
2. 1µm diamond on a medium nap, rayon flock cloth (Allied Final B)
3. ¼µm diamond on a medium nap, rayon flock cloth (Allied Final B)

6.5.3.3 Microscopy

A Nikon MA-200, inverted microscope, was employed for microscopy. The polished samples were inspected at various magnifications while all images were shot in bright-field at 200x magnification. Each image consisted of 4 images in the horizontal, stitched together, to provide a wider field-of-view. The approximate field-of-view for each image was 2050 µm x 450 µm.

6.5.3.4 Results

Changes were seen in the 285 K laser de-painted specimens 1 and 2 from the control specimen. Laser de-painted specimens showed cracks in the matrix, between fibers in fiber bundles, and through individual larger fibers near the surface. This is exemplified by comparing **Figures 28 and 29**.

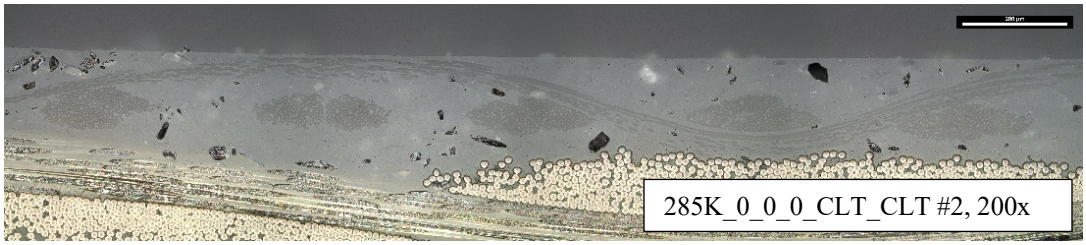

Figure 28 Cross Section of 285 K Control

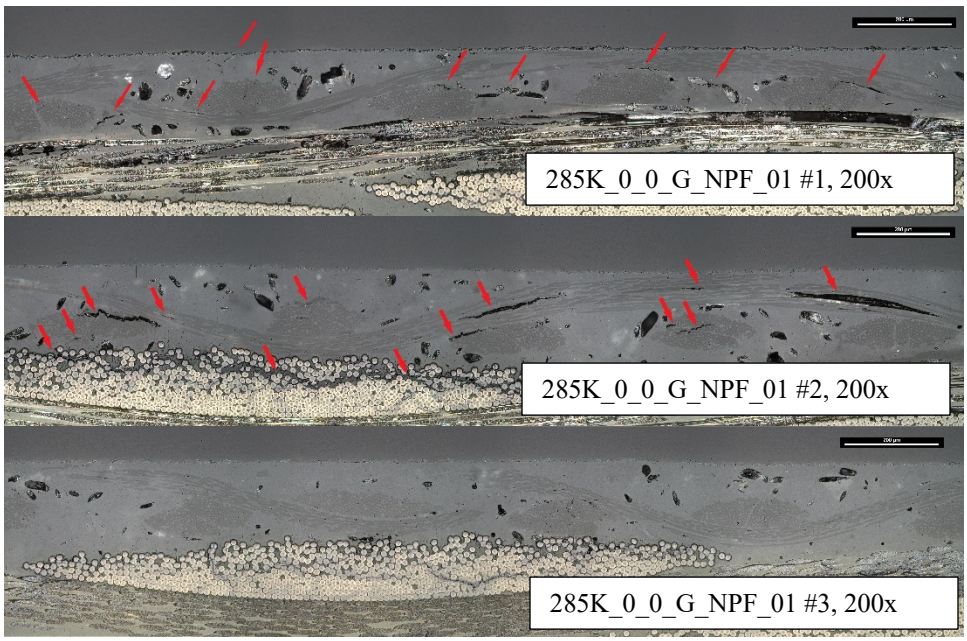

Figure 29 Cross Section of 285 K De-painted Panel

Minor changes were seen in the M46J_0_0_G_NPF laser de-painted panels. Damage is limited to the surface where minor separation of the epoxy from the fibers can be noticed, as well as, a few free-floating fibers, which are not present in the control panel (**Figures 30 and 31**).

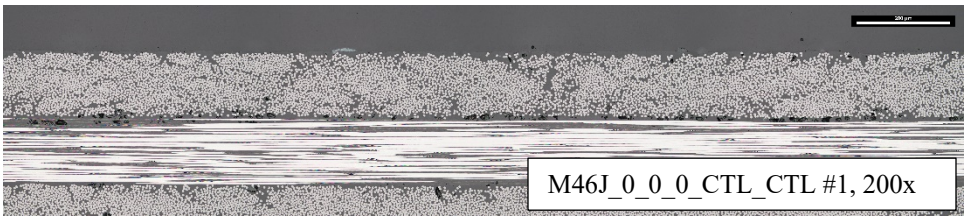

Figure 30 Cross Section of M46J Control Panel

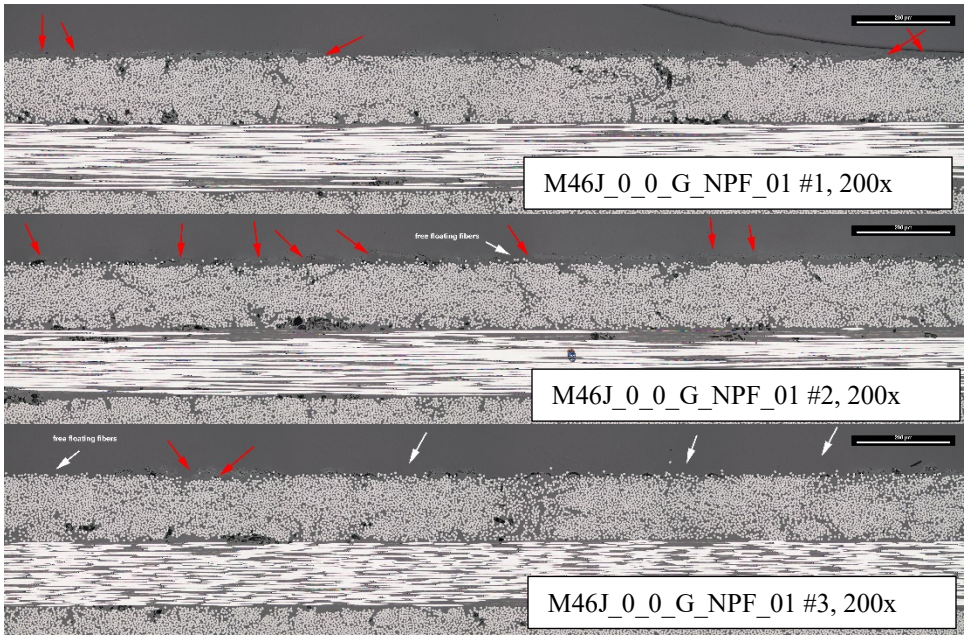

Figure 31 Cross Section of M46J G NPF De-painted Panel

No damage was found in the M46J_0_S_G_NPF_01 specimens. The surface sealer (which remained) had a fairly uniform coating of 130-150µm (5.12-5.9 mils) thick remaining on the surface. This likely protected the underlying substrate as shown in **Figure 32**.

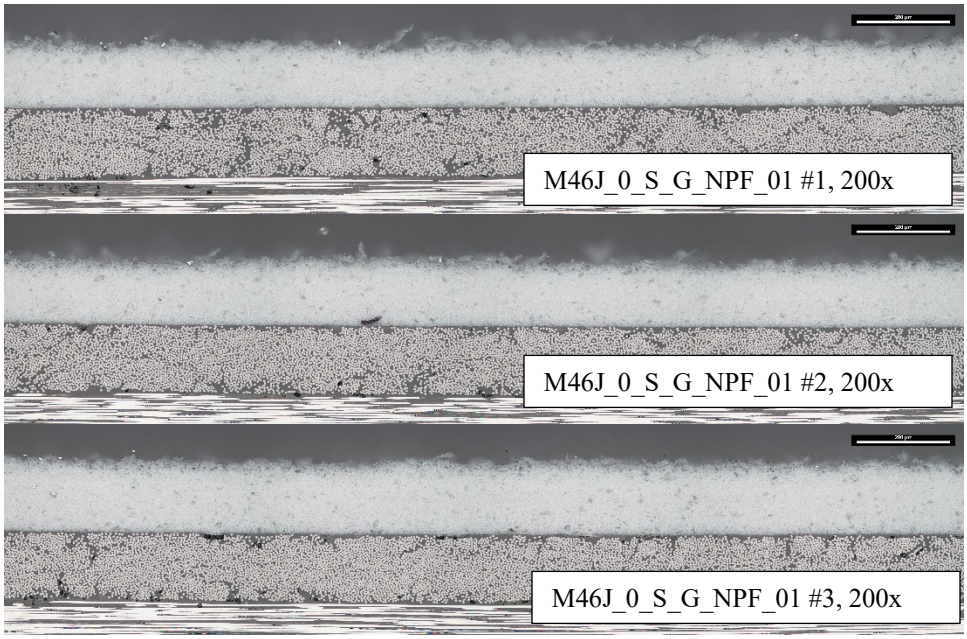

Figure 32 Cross Section of M46J S G NPF Control Panel

Damage was found in the M46J_0_0_GT_NPF_01 specimens. Specimen one had both free-floating fibers (white arrows) as well as separation of the resin from the fibers. This damage was observed to be close to the surface and under the paint layer (**Figure 33**).

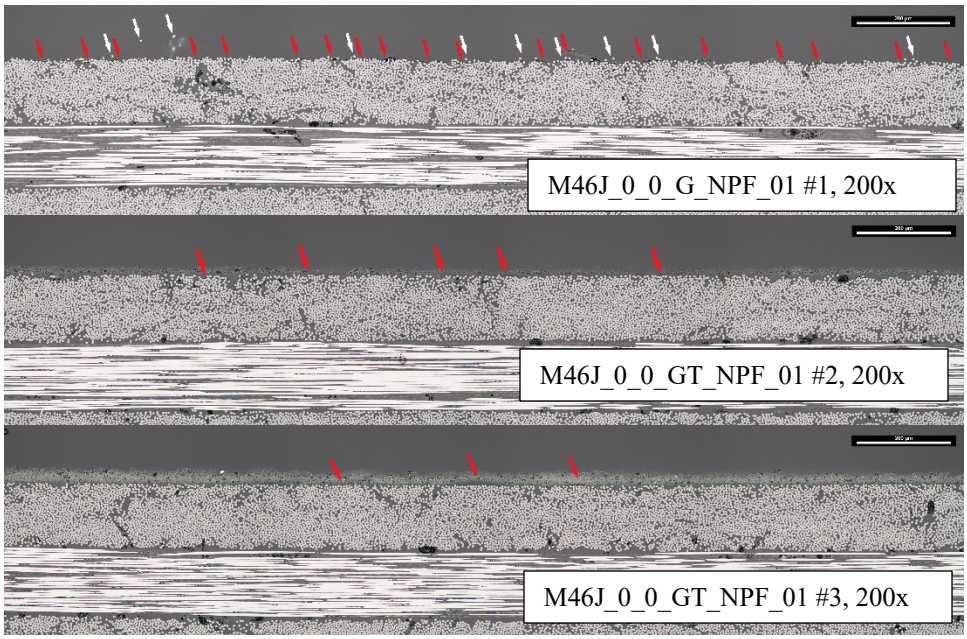

Figure 33 Cross Section of M46J GT NPF De-painted Panel

Damage was also found in the T650 de-painted specimens when compared to the control specimen in **Figure 34**. The resin can be seen to be separated from the fibers in all specimens in **Figure 35**.

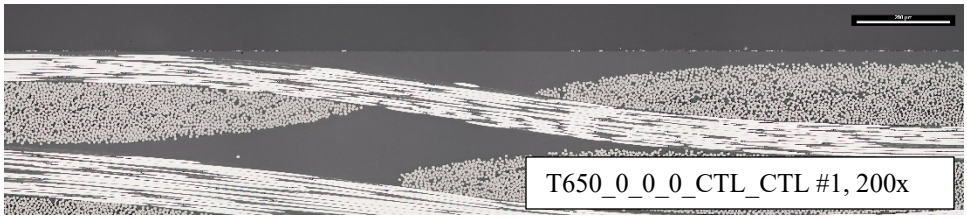

Figure 34 Cross Section of T650 Control Panel

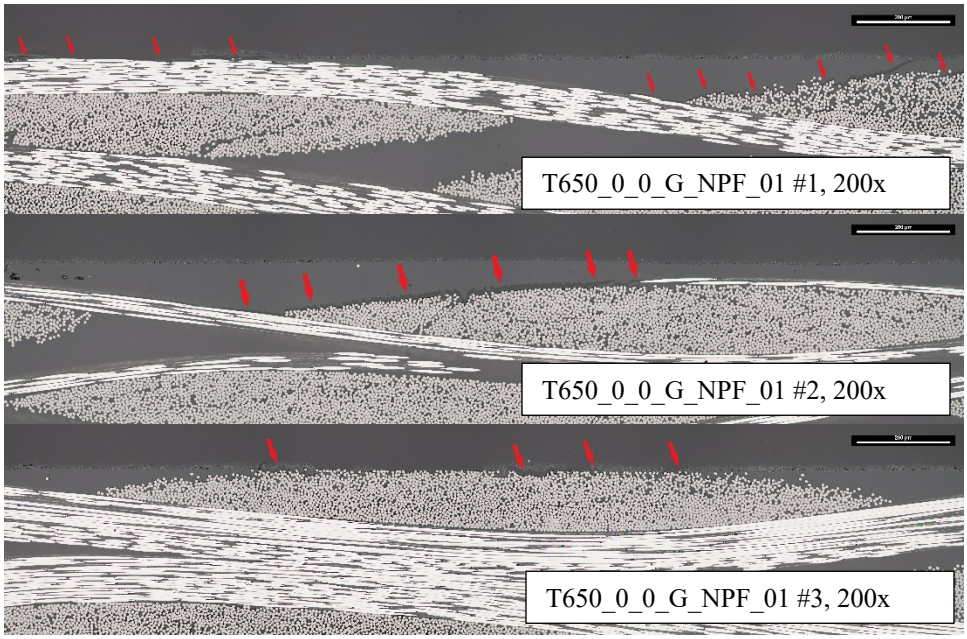

Figure 35 Cross Section of T650 De-painted Panel

In conclusion damage was found in all test conditions except the M46J_0_S_G_NPF_01 specimens with the surface sealer. The extent of the damage varies from surface damage and free-floating fibers to resin separation from the fibers deep in the composite. The impact of this damage was investigated in the long beam flexure testing.

6.5.4 Long Beam Flexure

Five samples were cut from each of the panels according to the cut plan as shown previously in **Figure 13.** Samples were tested in a four-point long beam flexure set up as shown in **Figure 36.**

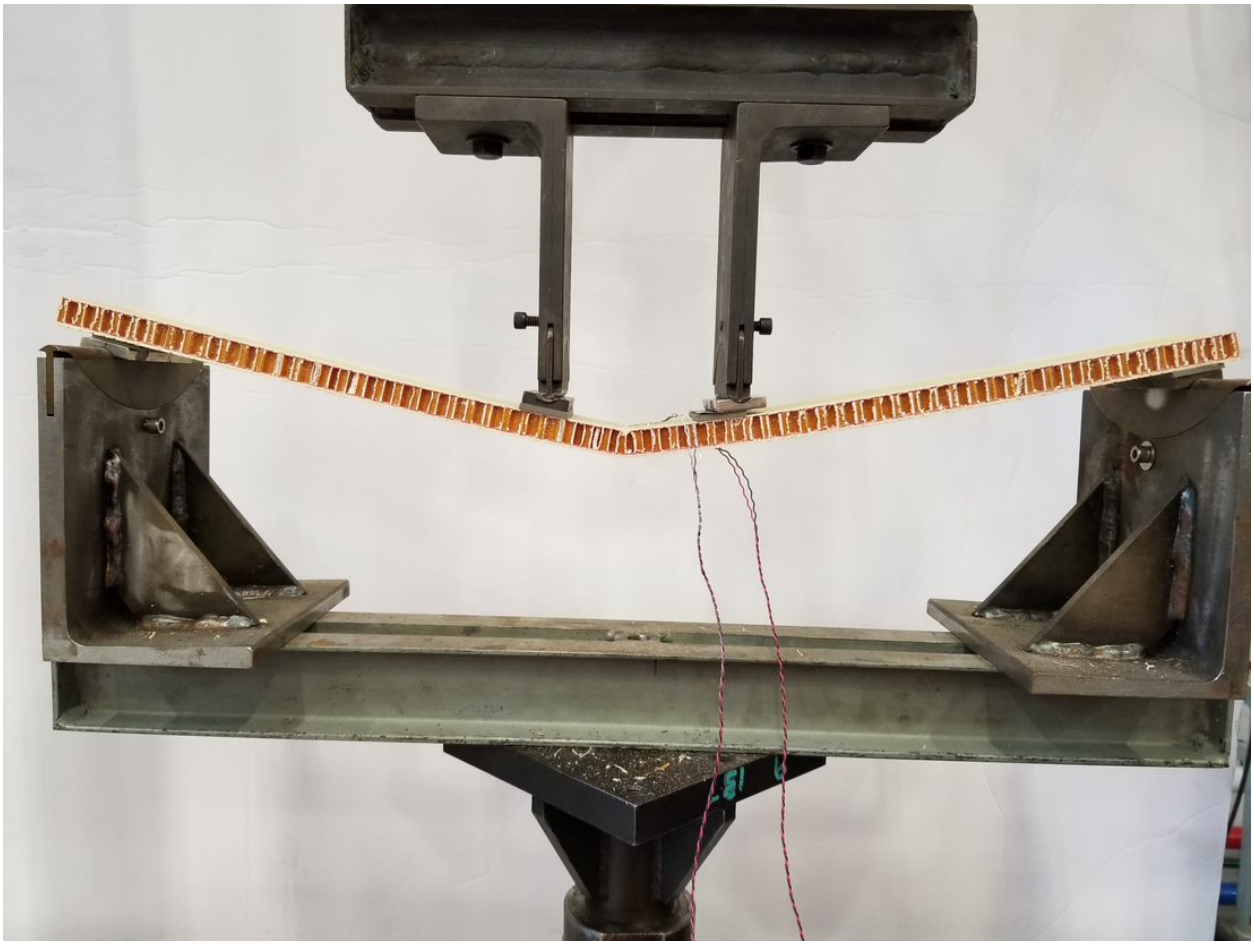

Figure 36 Four Point Long Beam Flexure Test

Long beam 4-point flexure testing (ASTM D7249/D7249M-18) was conducted on composite sandwich samples. The composite sandwiches were made of: a top facesheet that consisted of 2 plies, a honeycomb core, and then a bottom facesheet that consisted of 3 plies. A breakdown of the sandwich construction and corresponding sample IDs can be seen in **Table 30**. **Table 31** shows the results from the testing. The ribbon direction was arbitrarily chosen as the 0° direction on all panels since neither facesheet was marked properly during fabrication. We then assumed the fabric direction based on the ribbon direction. It is possible these were reversed. The direction on the plain weave and crow's foot fabrics also couldn't be determined.

Table 30 Sandwich Construction and Corresponding Sample IDs

Panel ID	Group	Ribbon Direction	2-Ply (Treated/Top)	3-Ply (Untreated/Bottom)	Cut Direction
M46J_0_S_G_NPF_01	2-Surfacer	0°	0°	0°	0°
M46J_0_0_GT_NPF_01	3-X4	0°	0°	0°	0°
M46J_0_0_0_CTL_CTL	5-None	0°	0°	0°	0°
M46J_0_0_G_NPF_01	1	0°	90°	90°	90°
T650_0_0_G_NPF_01	1-Prime/36173	0°	PW Fabric	PW Fabric	0°
T650_0_0_0-CTL-CTL	5-None	0°	PW Fabric	PW Fabric	0°
285K_0_0_G_NPF_01	1	0°	Crow's Foot/4HS	Crow's Foot/4HS	0°
285K_0_0_0-CTL-CTL	5-None	0°	Crow's Foot/4HS	Crow's Foot/4HS	0°

Table 31 Results Summary

Panel ID	Top Facesheet Ultimate Stress (ksi)	Bottom Facesheet Ultimate Stress (ksi)	Top Sheet Effective Chord Modulus (ksi)	Bottom Sheet Effective Chord Modulus (ksi)	Flexural Stiffness (lbf-in^2)
M46J_0_S_G_NPF_01	48.34 ± 2.64	40.22 ± 3.11	11,898.2 ± 230.0	18,339.5 ± 612.4	190,314 ± 3,088
M46J_0_0_GT_NPF_01	48.59 ± 5.04	37.82 ± 4.22	12,227.7 ± 236.5	19,783.2 ± 504.9	184,747 ± 2,621
M46J_0_0_0_CTL_CTL	58.64 ± 5.01	38.98 ± 2.41	12,655.3 ± 1,110.8	21,293.6 ± 1,978.9	178,977 ± 3,867
M46J_0_0_G_NPF_01	56.47 ± 6.27	42.79 ± 5.00	12,298.4 ± 1,008.9	19,766.7 ± 1,840.1	177,849 ± 5,285
T650_0_0_G_NPF_01	54.86 ± 4.12	39.45 ± 1.72	5,787.2 ± 115.1	8,666.9 ± 113.2	78,331 ± 1,259
T650_0_0_0-CTL-CTL	45.87 ± 2.60	39.95 ± 3.35	6,839.6 ± 650.2	10,449.5 ± 954.9	77,747 ± 1,022
285K_0_0_G_NPF_01	17.81 ± 0.98	15.17 ± 0.77	2,723.1 ± 121.9	3,702.0 ± 114.8	50,915 ± 815
285K_0_0_0-CTL-CTL	15.95 ± 1.76	13.28 ± 1.10	2,722.5 ± 63.2	3,690.0 ± 101.5	50,500 ± 658

Statistical analysis was performed on the results to determine if the change in results were significant. An F-test was performed to check for equal population variances. If the populations had equal variances, a T-test assuming equal variance was run at a 95% confidence interval. If the populations had unequal variances, a T-test assuming unequal variance was run, also at a 95% confidence interval. Statistical analysis results, summarized in **Table 32**, show two panels for which a process side statistical difference is found. This also shows three panels for which the unprocessed back side shows statistical difference. As such, further testing would be required to conclusively determine if the differences were due to the laser coating removal process. Associated graphs are captured in **Appendices B, C and D**.

Table 32 Statistical Analysis Results

		Ultimate Stress	Effective Chord Modulus	Flexural Stiffness
M46J_0_S_G_NPF_01	Top Facesheet (F^{u1}) (ksi)	No Statistical Difference from Control	No Statistical Difference from Control	No Statistical Difference from Control
	Bottom Facesheet (F^{u2}) (ksi)	No Statistical Difference from Control	Statistical Difference from Control	
M46J_0_0_GT_NPF_01	Top Facesheet (F^{u1}) (ksi)	No Statistical Difference from Control	No Statistical Difference from Control	No Statistical Difference from Control
	Bottom Facesheet (F^{u2}) (ksi)	No Statistical Difference from Control	No Statistical Difference from Control	
M46J_0_0_G_NPF_01	Top Facesheet (F^{u1}) (ksi)	No Statistical Difference from Control	No Statistical Difference from Control	Statistical Difference from Control
	Bottom Facesheet (F^{u2}) (ksi)	No Statistical Difference from Control	No Statistical Difference from Control	
T650_0_0_G_NPF_01	Top Facesheet (F^{u1}) (ksi)	Statistical Difference from Control	Statistical Difference from Control	No Statistical Difference from Control
	Bottom Facesheet (F^{u2}) (ksi)	No Statistical Difference from Control	Statistical Difference from Control	
285K_0_0_G_NPF_01	Top Facesheet (F^{u1}) (ksi)	No Statistical Difference from Control	No Statistical Difference from Control	No Statistical Difference from Control
	Bottom Facesheet (F^{u2}) (ksi)	Statistical Difference from Control	No Statistical Difference from Control	

7.0 COST ASSESSMENT

A cost-benefit analysis was not generated for this project.

7.1 Cost Model

A cost model was not created for this project.

7.2 Cost Analysis and Comparison

Cost analysis and comparison were not provided on this project.

8.0 IMPLEMENTATION ISSUES

Southwest Research Institute (SwRI) had the original subcontract and work effort that lasted approximately five months. There were project delays and issues that resulted in the decision by AFLCMC/EZP on February 18, 2018 to relocate the 1 kW NSP laser system to UDRI. The laser was then shipped to Titan Robotics in Pittsburgh, Pennsylvania.

Scope change was a consistent problem throughout the program. The original proposal was created for composite panel testing, which then changed to include metallic panels because they were cheaper and faster to purchase for the program. The procurement of the composite panels was extremely complex because of security concerns for purchasing the pieces and parts. Therefore, parts had to be purchased separately and then shipped to another vendor for assembly. It was a nine month process to purchase and build the required number of composite panels required for the program.

The proposed testing included the use of a Lincoln Polytek Polygon scanner with the 1 kW NPF laser system. The Lincoln Polytek Polygon scanner proved to be too large and cumbersome for use on the end effector and was ultimately replaced with a Galvanometer (GALVO) scanner.

The program was stopped prior to the end of the period of performance because of another request to change the scope. The original purpose of the program was to test the 1 kW NPF scanner. The last request for scope change included the qualification of a 10 kW continuous wave scanner. The ESTCP review board then decided to end the program and to have UDRI return funding that had not been previously spent.

9.0 REFERENCES

ACS-MRS-5002 *Carbon Fiber, Epoxy Impregnated, 250 Degree F Cure, High Modulus, Moderate Impact Resistant.* Northrup Grumman, May 2017.

ASTM D3359 *Standard Test Methods for Measuring Adhesion by Tape Test.* March 2017.

ASTM D4541 *Standard Test Method for Pull-Off Strength of Coating Using Portable Adhesion Testers.* August 2017.

ASTM D7127 *Standard Test Method for Measurement of Surface Roughness of Abrasive Blast Cleaned Metal Surface Using a Portable Stylus Instrument.* December 2017.

ASTM D7249 *Facing Properties of Sandwich Constructions by Long Beam Flexure.* April 2017.

ASTM E3 *Standard Guide for Preparation of Metallographic Specimens.* June 2017.

ASTM E7 *Standard Terminology Relating to Metallography.* July 2017.

ASTM E8 *Standard Test Methods for Tension Testing of Metallic Materials.* February 2020.

ASTM E18 *Standard Test Methods for Rockwell Hardness of Metallic Materials.* October 2018.

ASTM E466 *Standard Practice for Conducting Force Controlled Constant Amplitude Axial Fatigue Tests of Metallic Materials*. July 2015.

MILA-8625 *Anodic Coating for Aluminum and Aluminum Alloys.* Version F, September 1993.

MIL-C-5541 *Military Specification: Chemical Conversion Coatings on Aluminum and Aluminum Alloys.* Version E, November 1990.

MIL-DTL-5541 *Detail Specification: Chemical Conversion Coatings on Aluminum and Aluminum Alloys.* Version F, July 2006.

MIL-PRF-85285 *Military Performance Specification: Coating: Polyurethane, Aircraft and Support Equipment.* Version E, January 2012.

MIL-PRF-23377 *Military Performance Specification: Primer Coatings Epoxy, High-Solids.* Version K, June 2012.

MIL-STD-1537 *Military Standard: Test Method Standard for Electrical Conductivity Test for Verification for Heat Treatment of Aluminum Alloys Eddy Current Method.* Version C, June 2002.

SAE J442 *Test Strip, Holder, and Gage for Shot Peening.* February 2013.

SAE MA4872A *Paint Stripping of Commercial Aircraft – Evaluation of Materials and Processes.* November 2012.

STM22-817 *Material Specification Wovern Carbon/Epoxy Fabric, 350°F Cure for 220°F Applications.* Lockheed Martin Aeronautics Company, Revision B, May 2018.

STM22-912 *Material Specification Epoxy Impregnated Aramid Fiber Fabric, 250°F.* Lockheed Martin Aeronautics Company, Revision F, October 2006.

TO 1-1-8 *Technical Manual: Application and Removal of Organic Coatings, Aerospace and Non-Aerospace Equipment.* January 2010 with Change 26, October 2019.

APPENDICES

Appendix A: Points of Contact

POINT OF CONTACT Name	ORGANIZATION Name Address	Phone Fax E-mail	Role in Project
Randall Straw	AFLCMC/EZP BLDG 30070 Wright-Patterson Air Force Base, OH 45433	937-470-4451 Randall.straw.1@us.af.mil	Program Manager
Jesse Holdaway	Carnegie Mellon 5000 Forbes Ave, Pittsburgh, PA 15213	801-707-5645 Jesse.holdaway@cmu.edu	Program Manager
Connor Eviston	AFLCMC/RO, 4375 Chidlaw Dr, Wright-Patterson Air Force Base, OH 45433	937-668-1050 Connor.eviston.1@us.af.mil	Program Manager
Chris Venturella	UDRI 1700 S. Patterson Blvd Dayton, OH 45409	419-296-5896 Chris.venturella@udri.udayton.edu	Laser Engineer
Hannah Easton	UDRI 1700 S. Patterson Blvd Dayton, OH 45409	937-708-9964 Hannah.easton@udri.udayton.edu	Laser Engineer
Bryan Pavlich	UDRI 1700 S. Patterson Blvd Dayton, OH 45409	937-229-4011 Bryan.Pavlich@udri.udayton.edu	Project Manager
Natalia Voevodin	UDRI 1700 S. Patterson Blvd Dayton, OH 45409	937-668-2631 Natalia.voevodin@udri.udayton.edu	Sr. Research Scientist
Andy Strat	Titan Robotics 2516 Jane St. Pittsburgh, PA 15203	703-965-5760 andy@titanrobots.com	Robotics Engineer

Appendix B: Ultimate Stress Graph

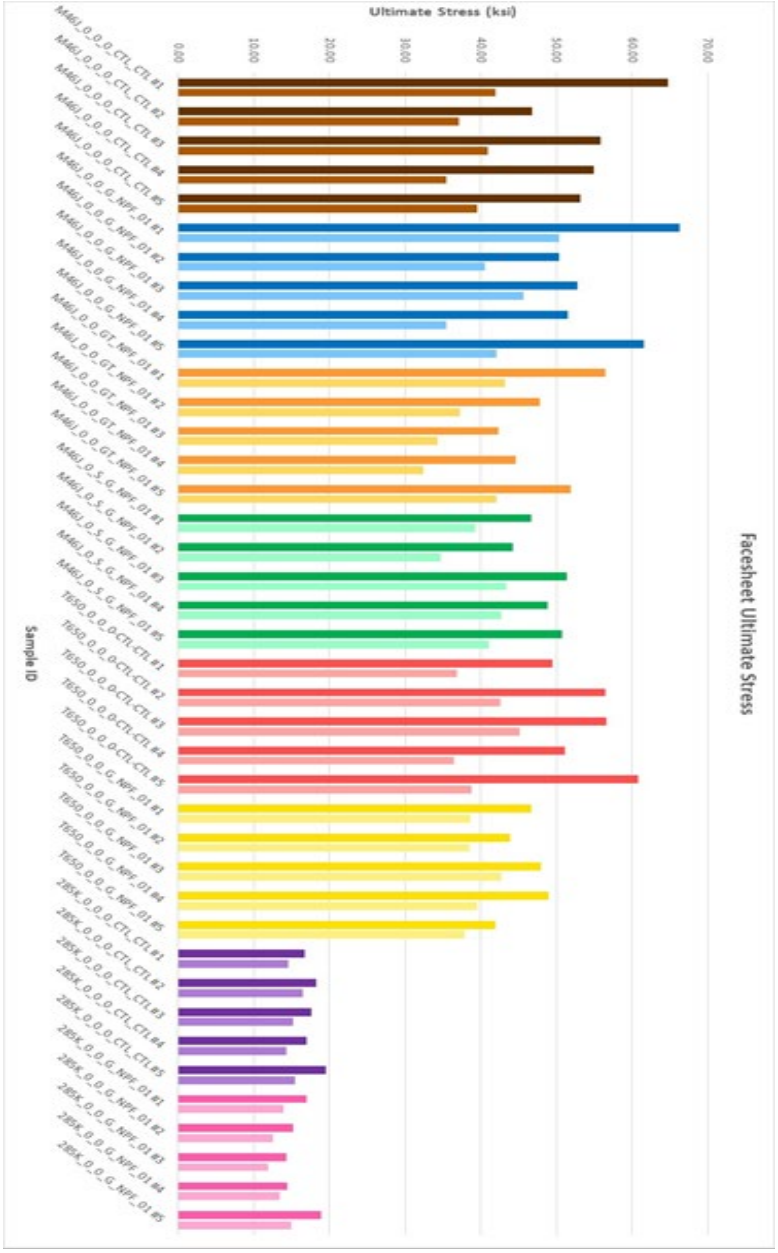

Appendix C: Chord Modulus Graph

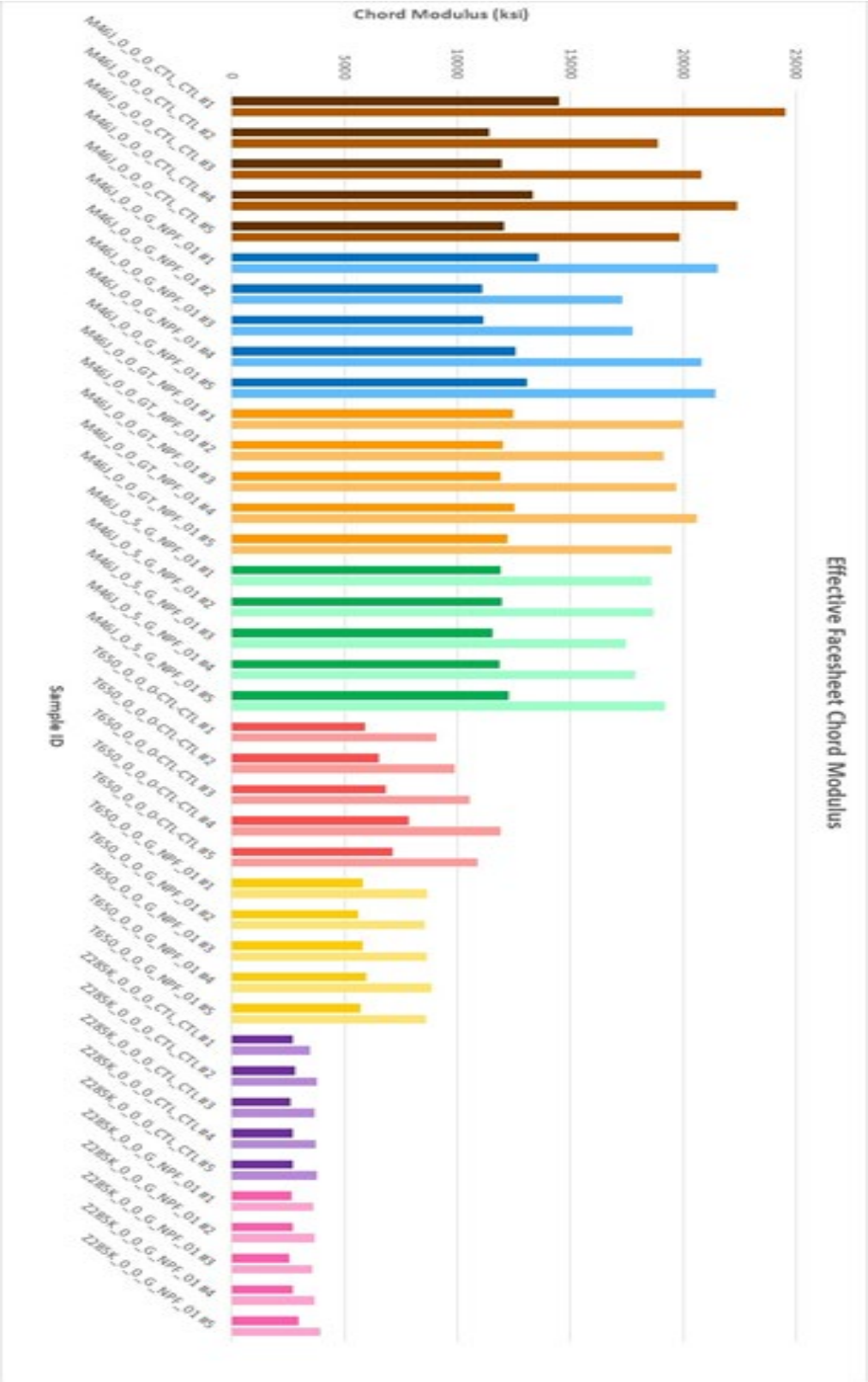
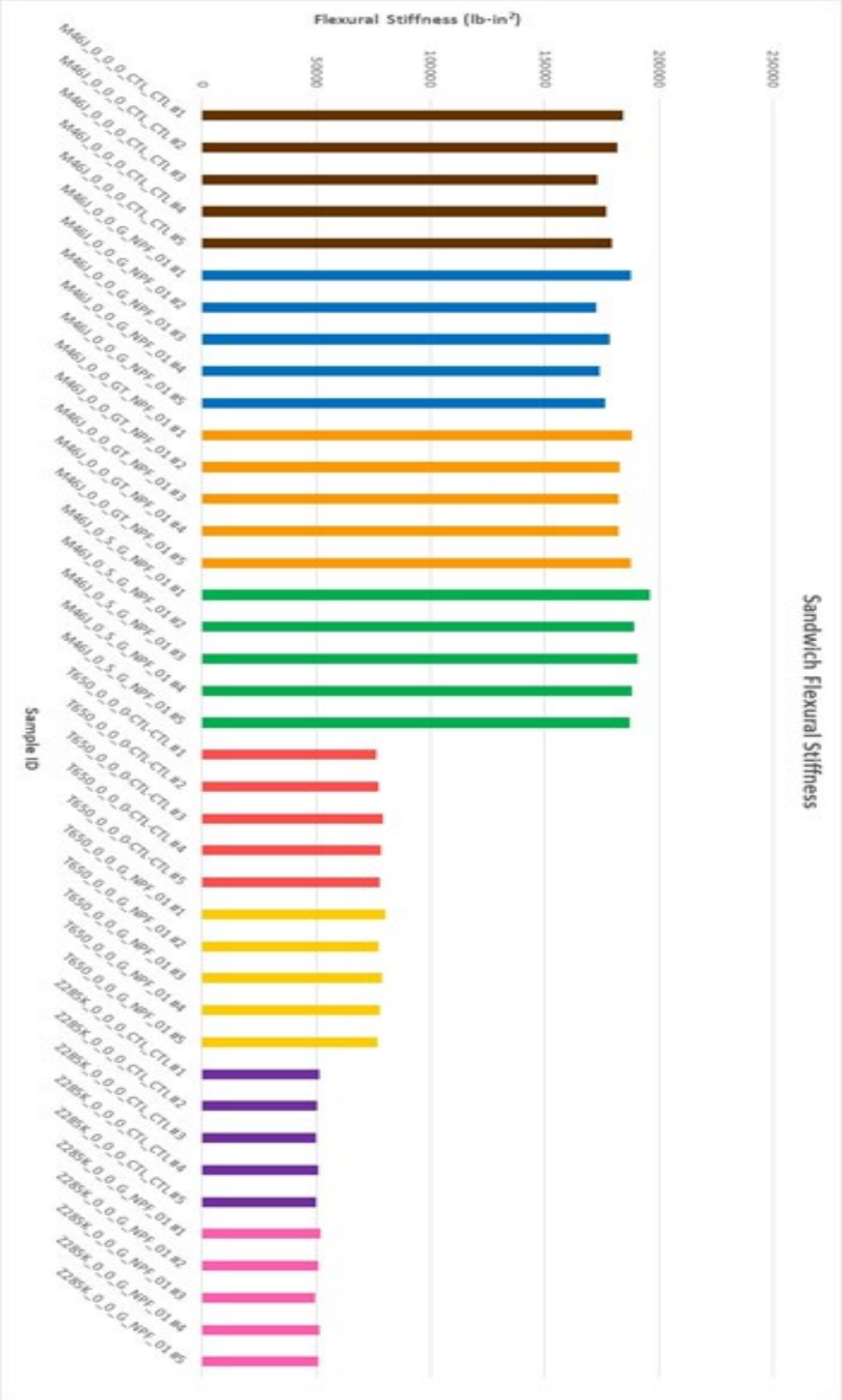
Appendix D: Flexural Stiffness Graph